



Measurement of the muon anomalous magnetic moment with the Fermilab g-2 experiment

Saskia Charity, University of Liverpool

Birmingham EPP Seminar, 06 December 2023

Muons & magnetic moments

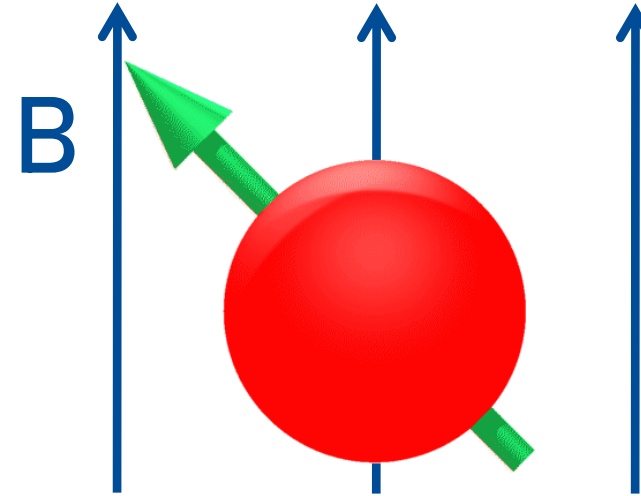
g determines spin precession frequency in a magnetic field

Torque in B-field

$$\vec{\mu} \times \vec{B}$$

Magnetic Moment

$$\vec{\mu} = g \frac{e}{2m} \vec{S}$$



Muons & magnetic moments

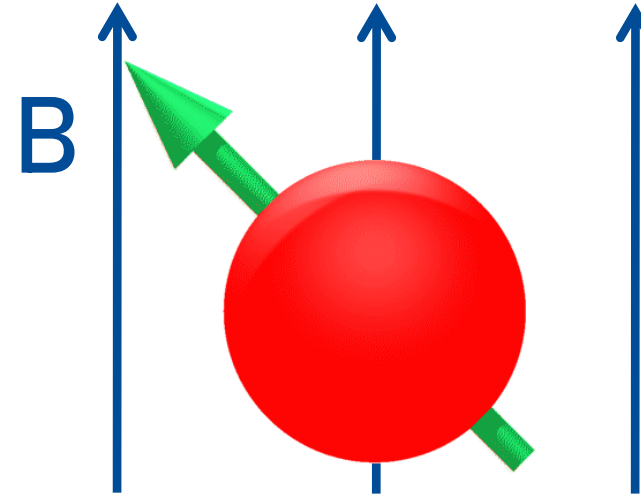
g determines spin precession frequency in a magnetic field

Torque in B-field

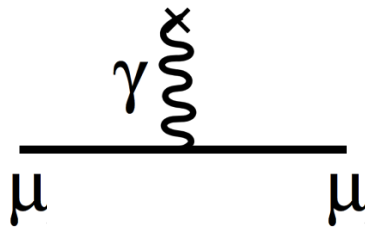
$$\vec{\mu} \times \vec{B}$$

Magnetic Moment

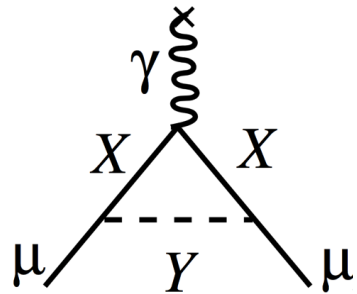
$$\vec{\mu} = g \frac{e}{2m} \vec{S}$$



$$g = 2$$



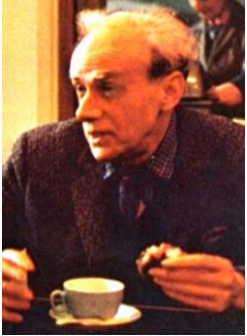
$$g > 2$$



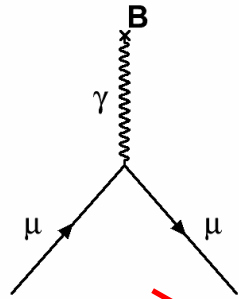
- For a pure Dirac spin- $\frac{1}{2}$ charged fermion, g is exactly 2
- Interactions between the muon and **virtual particles** alter the value: X & Y particles could be SM or new physics

Standard Model components of g_μ

Dirac



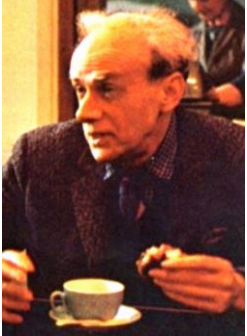
Charged,
spin $\frac{1}{2}$



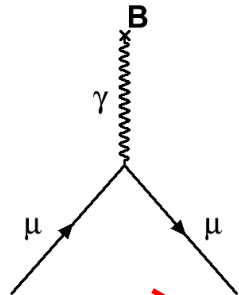
$$g_\mu^{SM} = 2$$

Standard Model components of g_μ

Dirac

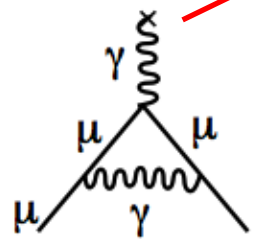
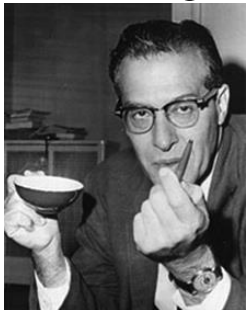


Charged,
spin $\frac{1}{2}$



$$g_\mu^{SM} = 2.0023$$

Schwinger

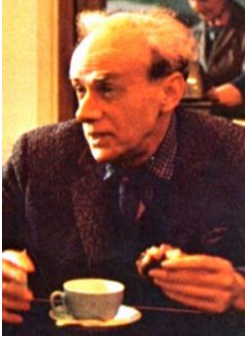


1st Order QED

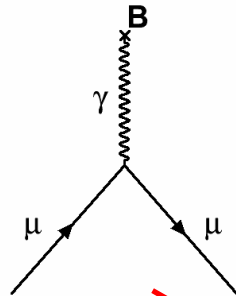
$$\frac{\alpha}{2\pi} = 0.00232$$

Standard Model components of g_μ

Dirac



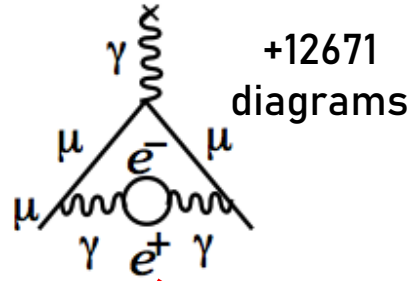
Charged,
spin $\frac{1}{2}$



Kinoshita

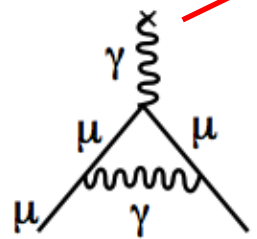
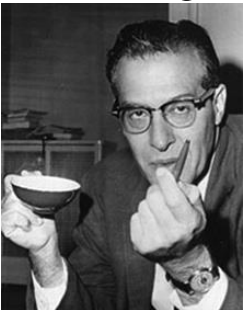


Up to 10th
Order QED



$$g_\mu^{SM} = 2.002331$$

Schwinger

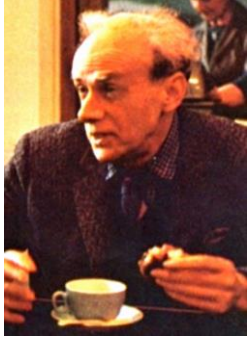


1st Order QED

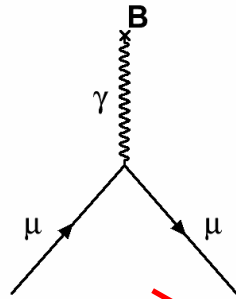
$$\frac{\alpha}{2\pi} = 0.00232$$

Standard Model components of g_μ

Dirac



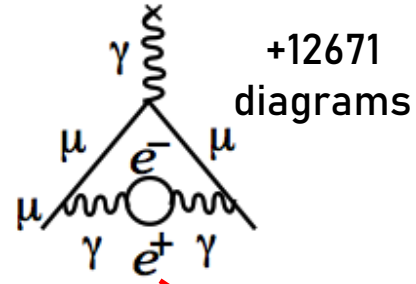
Charged,
spin $\frac{1}{2}$



Kinoshita



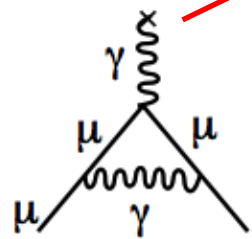
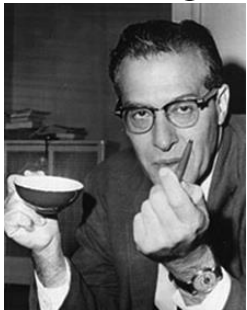
Up to 10th
Order QED



$$g_\mu^{SM} = 2.00233183$$

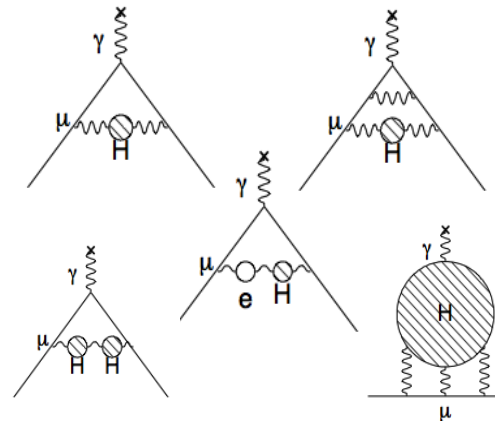
Hadronic

Schwinger



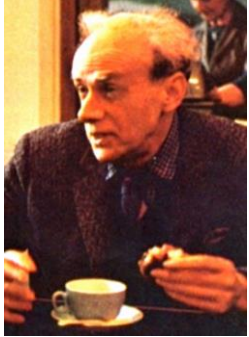
1st Order QED

$$\frac{\alpha}{2\pi} = 0.00232$$

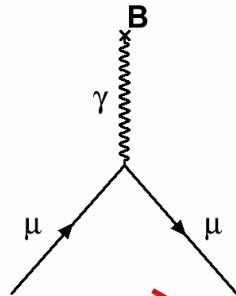


Standard Model components of g_μ

Dirac



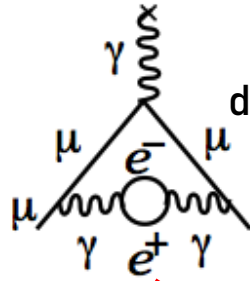
Charged, spin 1/2



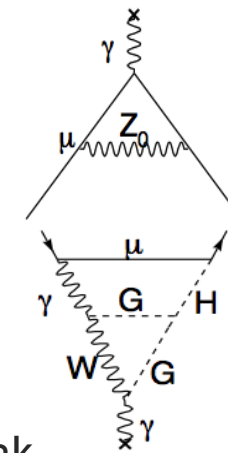
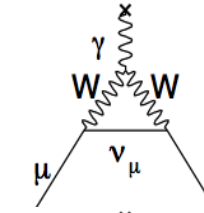
Kinoshita



Up to 10th Order QED



+12671 diagrams

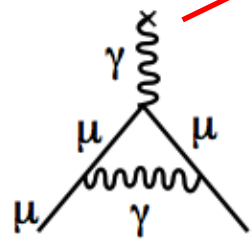
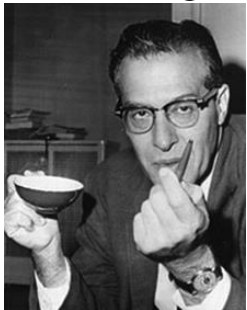


Electroweak

$$g_\mu^{SM} = 2.0023318362$$

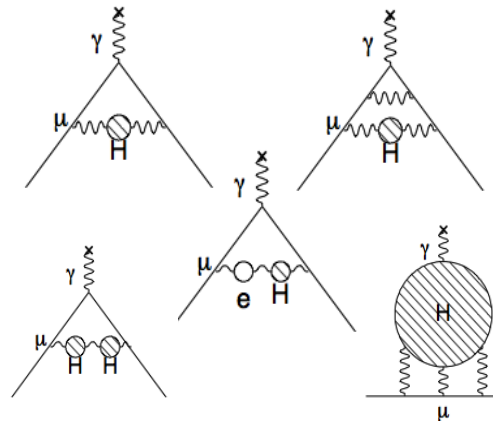
Hadronic

Schwinger



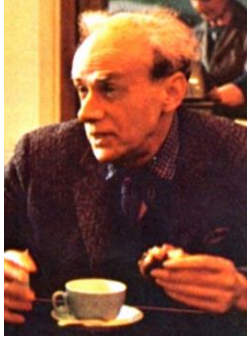
1st Order QED

$$\frac{\alpha}{2\pi} = 0.00232$$

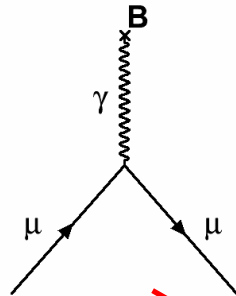


Standard Model components of g_μ

Dirac



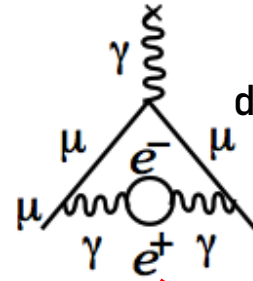
Charged,
spin $\frac{1}{2}$



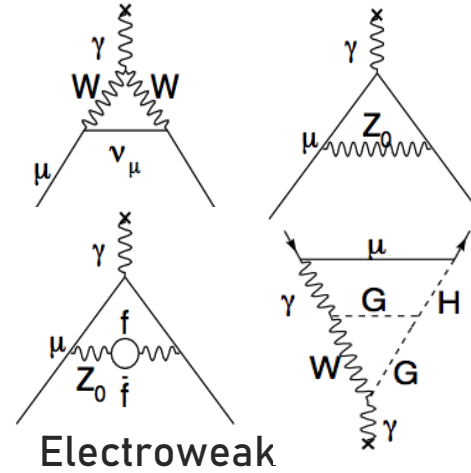
Kinoshita



Up to 10th
Order QED



+12671
diagrams



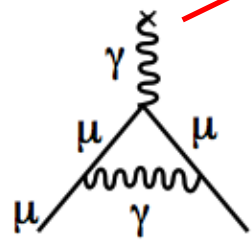
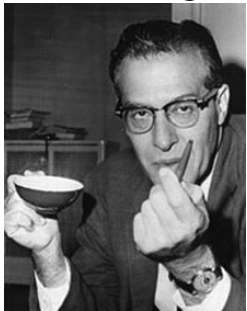
Electroweak

$$g_\mu^{SM} = 2.00233183620(86)$$

Hadronic

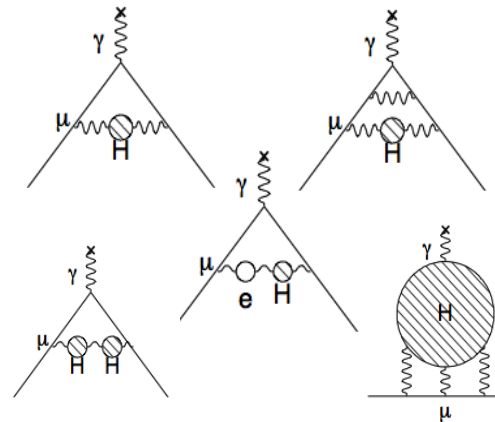
BSM?

Schwinger

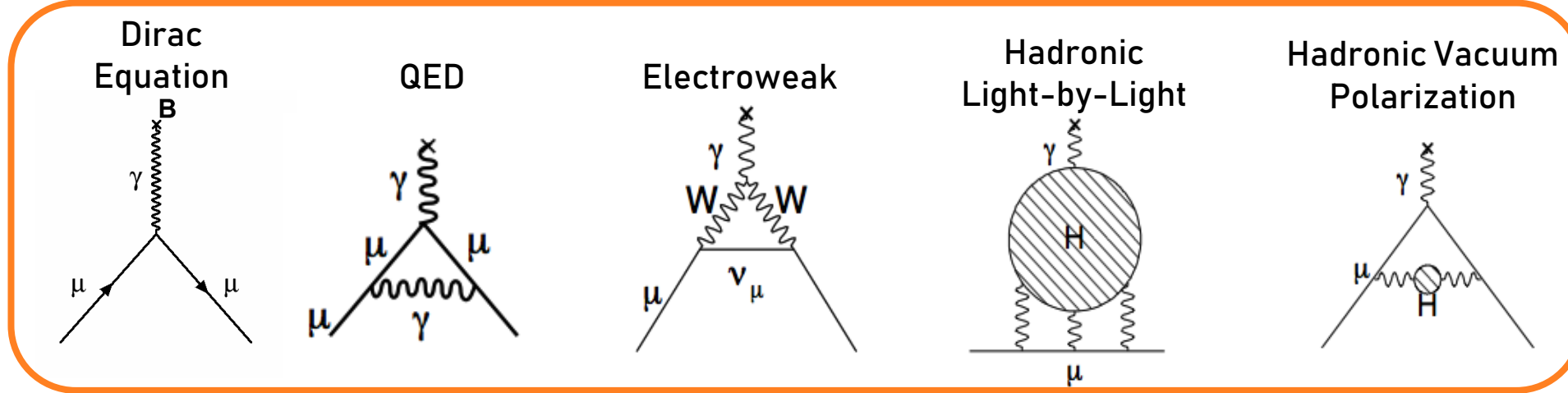


1st Order QED

$$\frac{\alpha}{2\pi} = 0.00232$$



Muon $g-2$ Theory Initiative



- SM values taken from the **Muon $g-2$ Theory Initiative**



TI in Bern, September 2023

- Consortium of 100+ theorists who compile the theoretical inputs and provide recommendations
- Last compilation in **2020**:

White Paper: Phys. Rept. 887 (2020) 1-166
<https://doi.org/10.1016/j.physrep.2020.07.006>

<https://muon-gm2-theory.illinois.edu/>

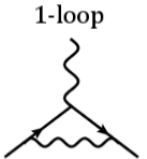
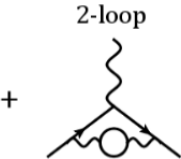
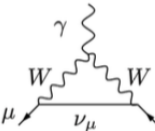

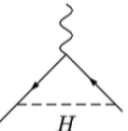
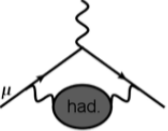

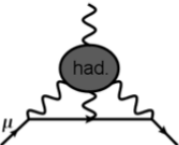
The muon anomalous magnetic moment

- Define the quantity a_μ : muon anomalous magnetic moment

$$a_\mu = \frac{g_\mu - 2}{2}$$

- a_μ arises due to higher-order interactions/loop contributions
- All SM particles contribute
- Calculate & sum all sectors of the SM

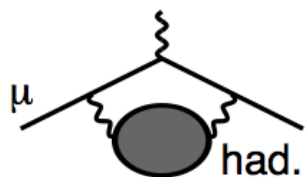
$$a_\mu^{\text{SM}} = a_\mu^{\text{QED}} + a_\mu^{\text{EW}} + a_\mu^{\text{HVP}} + a_\mu^{\text{HLbL}}$$

	1-loop	2-loop		a_μ^{SM} portion	δa_μ^{SM} portion	
QED			...	Perturbative (Known to five-loop)	~ 99.99%	~0.001%
EW				Perturbative (Known to two-loop)	~ 1 ppm	~0.2%
HVP				Non-perturbative (Data-driven & lattice)	~ 59 ppm	~84%
HLbL				Non-perturbative (Data-driven & lattice)	~ 1 ppm	~16%

QED dominates the value

Hadronic terms dominate the uncertainty

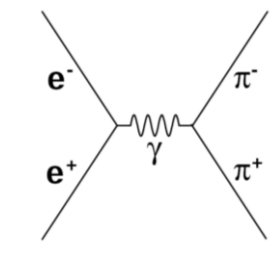
Hadronic Vacuum Polarisation (HVP): dispersion relation



$a_{\mu}^{\text{had,LO}}$

Dispersion Relation
follows from causality

$$\text{had.} = \int \frac{ds}{\pi(s-q^2)} \text{Im had.}$$



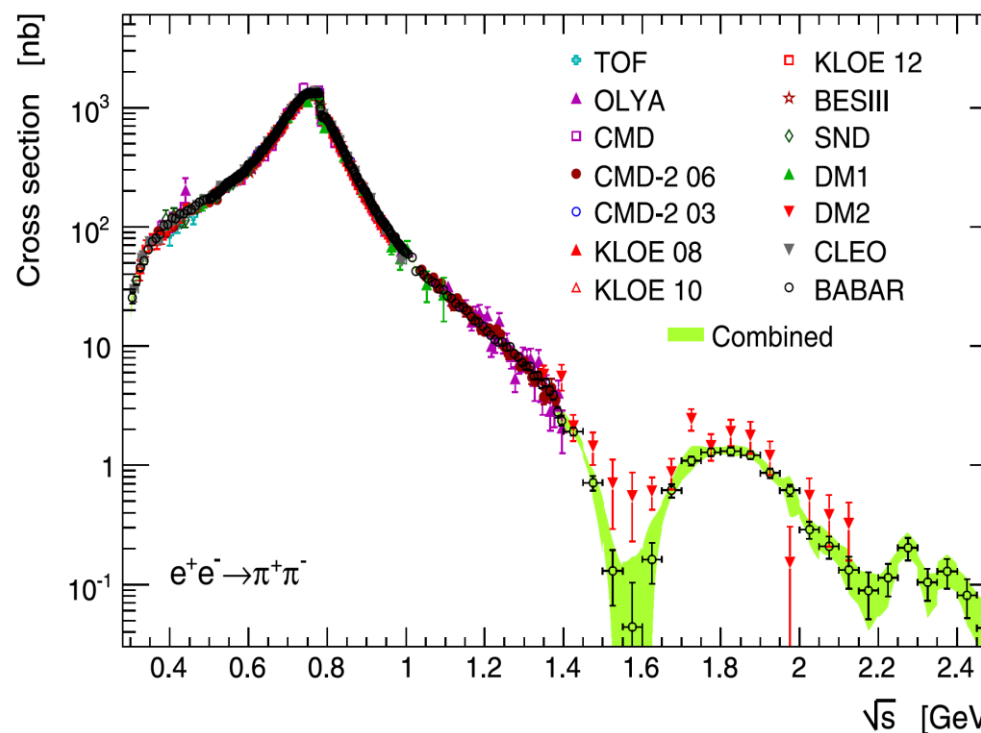
Optical Theorem
follows from unitarity
of scattering matrix

$$2 \text{Im had.} = \sum_{\text{had.}} \int d\Phi \left| \text{had.} \right|^2$$

$$a_{\mu}^{\text{had,LO}} = \frac{m_{\mu}^2}{12\pi^3} \int_{s_{\text{th}}}^{\infty} ds \frac{1}{s} \hat{K}(s) \sigma_{\text{had}}(s)$$

- $1/s$ weight \rightarrow low energies most important
- $\pi^+\pi^-$ contributes 73% to LO
- Need to know total hadronic cross-section $\sigma_{\text{had}}(s)$

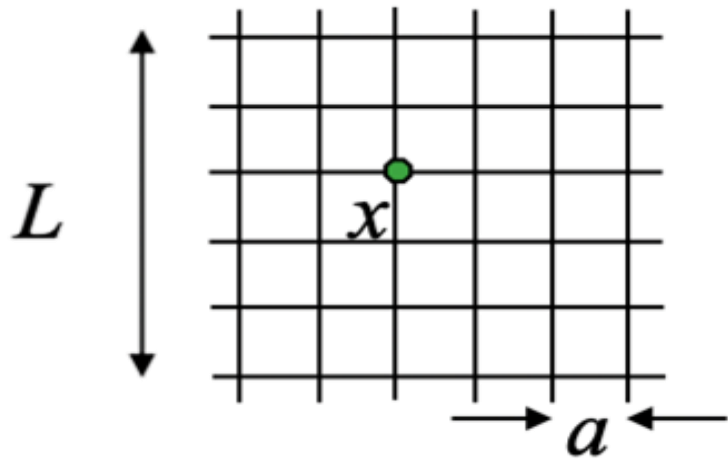
Cross section data used in TI 2020 a_{μ}^{HVP} prediction



Davier et. al, Eur. Phys. J. C. 80 (2020)

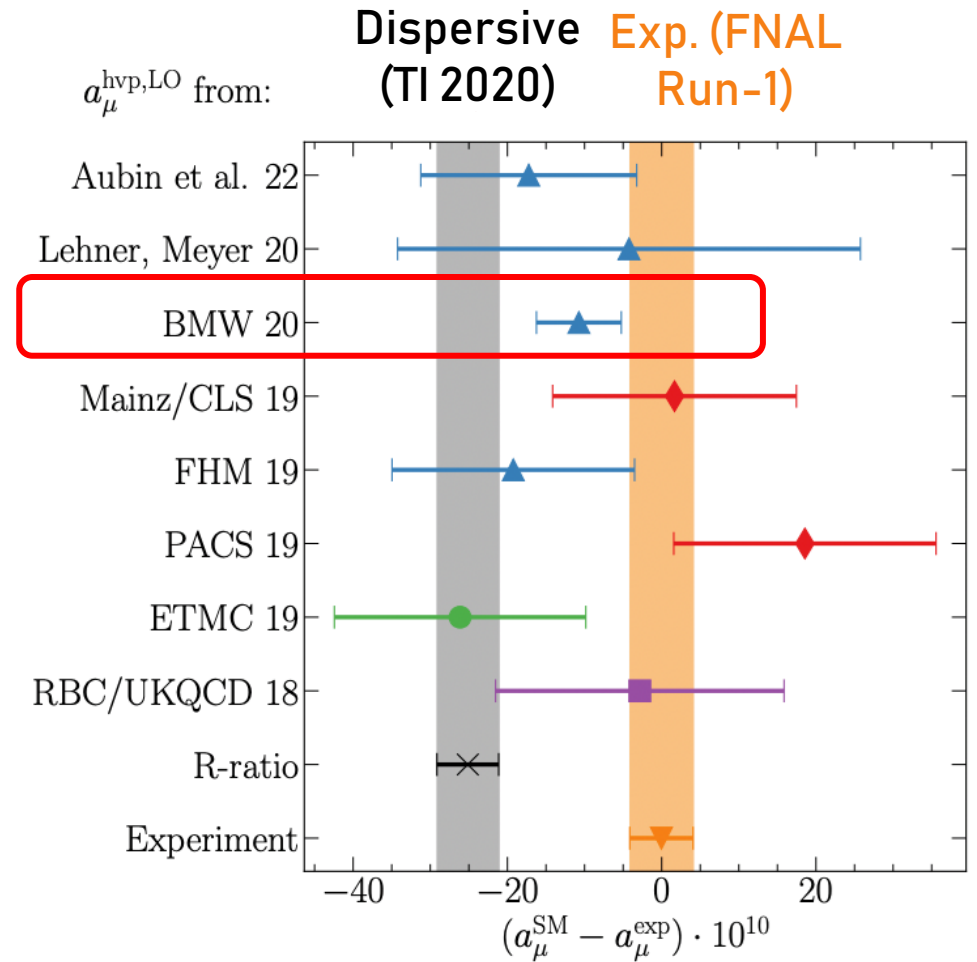
Hadronic Vacuum Polarisation (HVP): lattice approach

- First principle calculation to predict a_μ
- Numerical integration on finite space-time lattice \rightarrow very computationally expensive



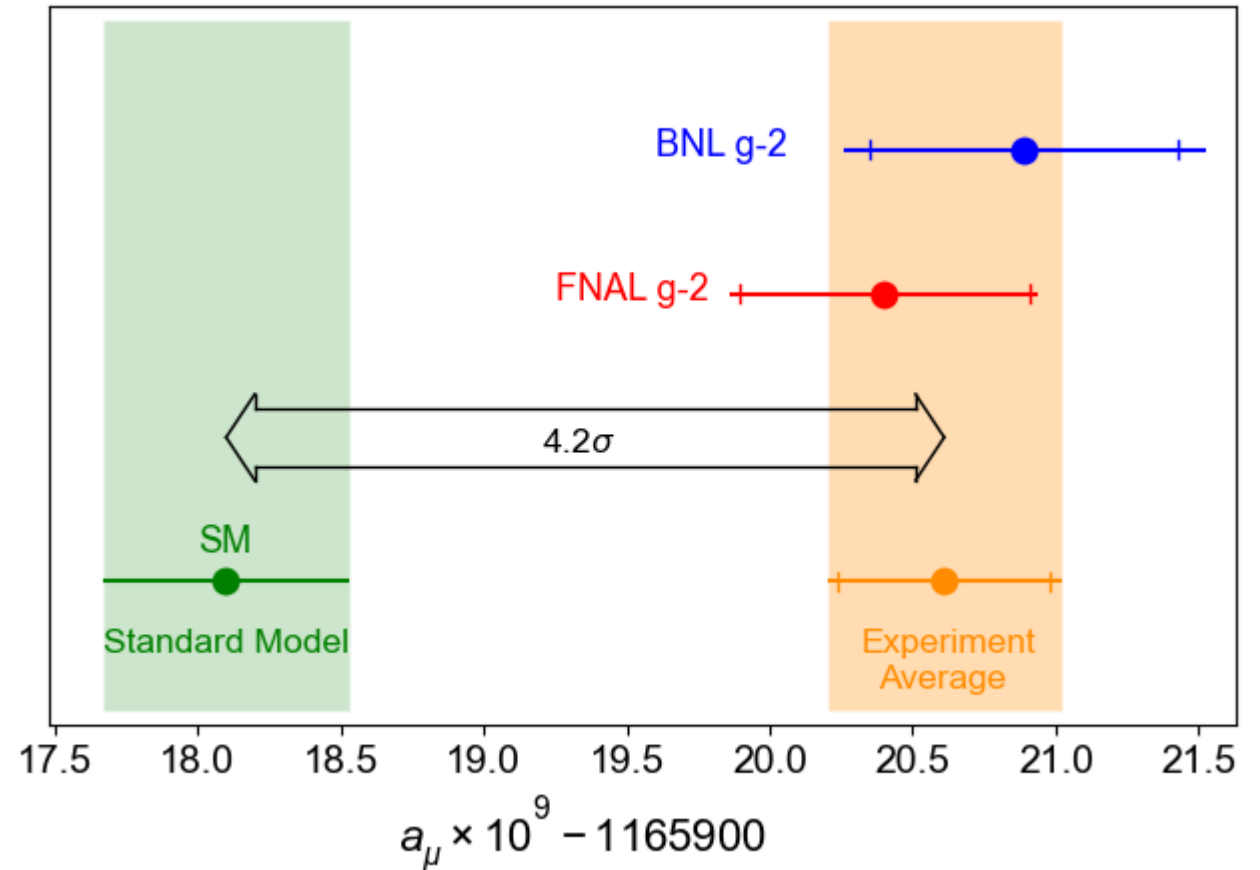
First prediction
with <1%
uncertainty by
BMW

- Lattice results not included in TI 2020 white paper due to low precision
- So far, no other high-precision a_μ from different group
- Ongoing cross-checks by many groups at different energies
- Preliminary agreement in 'intermediate energy window'



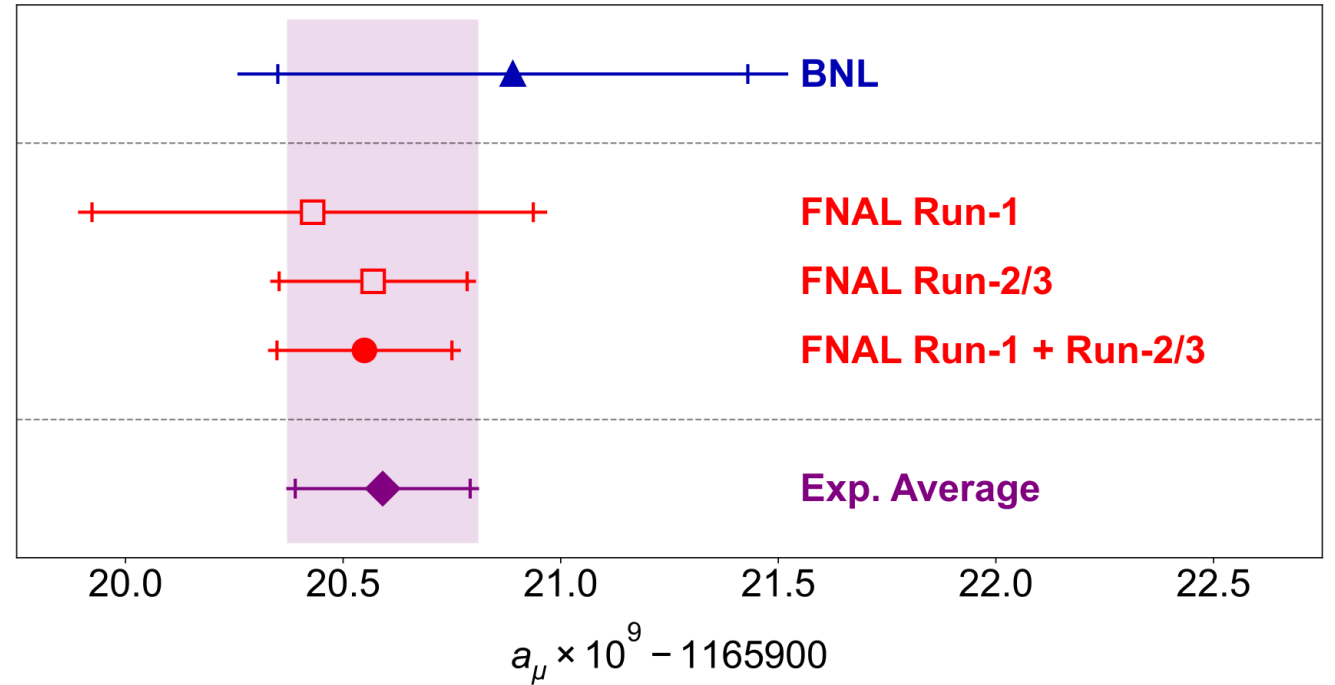
FNAL Measurement: status in 2021

- First announcement of the FNAL experiment using Run-1 (2018) data in April 2021
- Using the TI(2020) value for the SM comparison (data-driven HVP only)



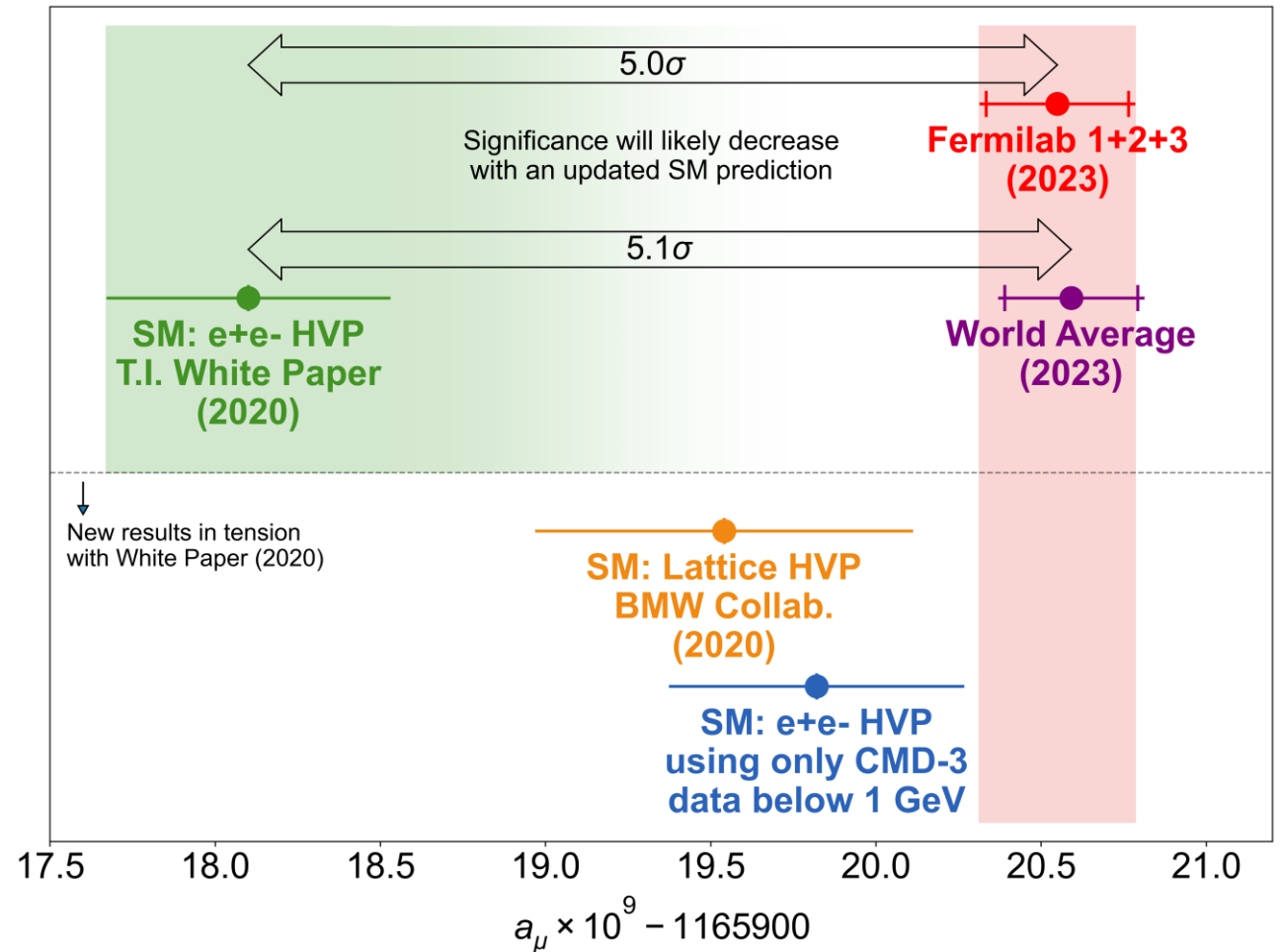
FNAL Measurement: status in 2023

- In August 2023, FNAL published updated result using Run-2 (2019) and Run-3 (2020) data
- >4x higher statistics than the Run-1 result
- Excellent agreement with Run-1 and BNL
- BNL, Run-1 and Run-2/3 statistics dominated
- Assume 100% correlated systematics
- World Average dominated by FNAL

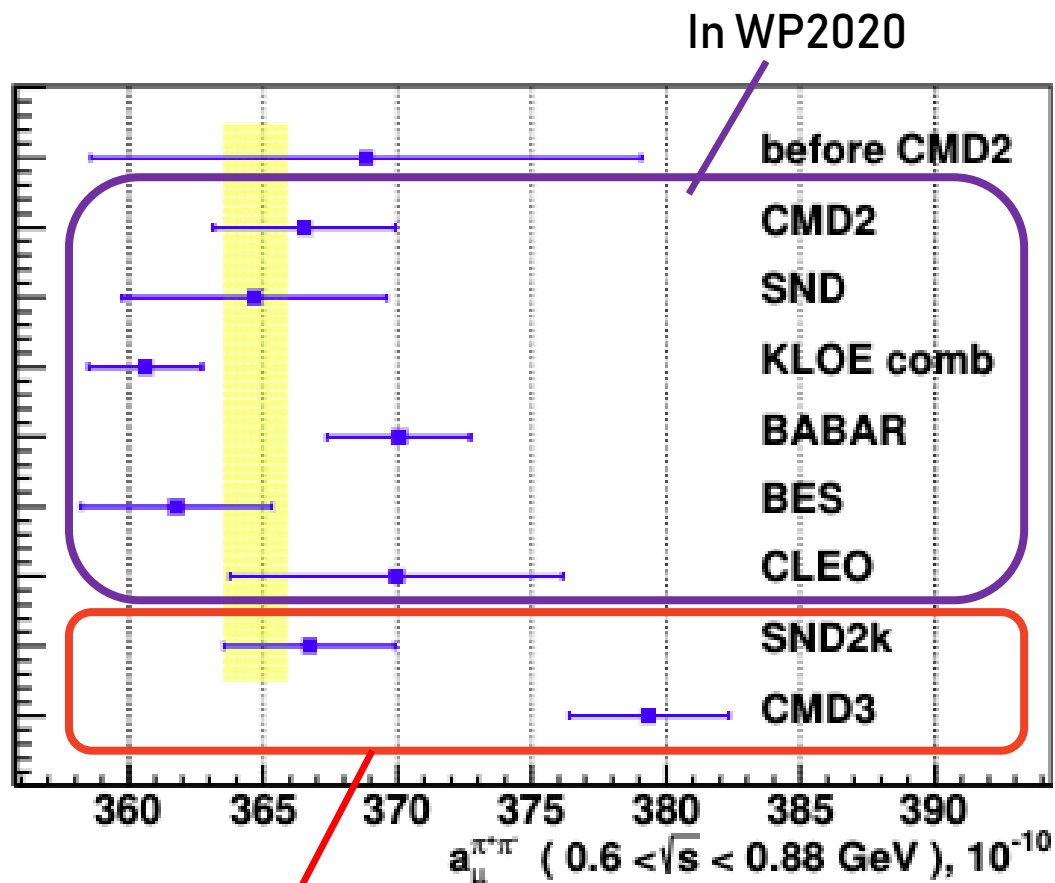


Comparison with the Standard Model

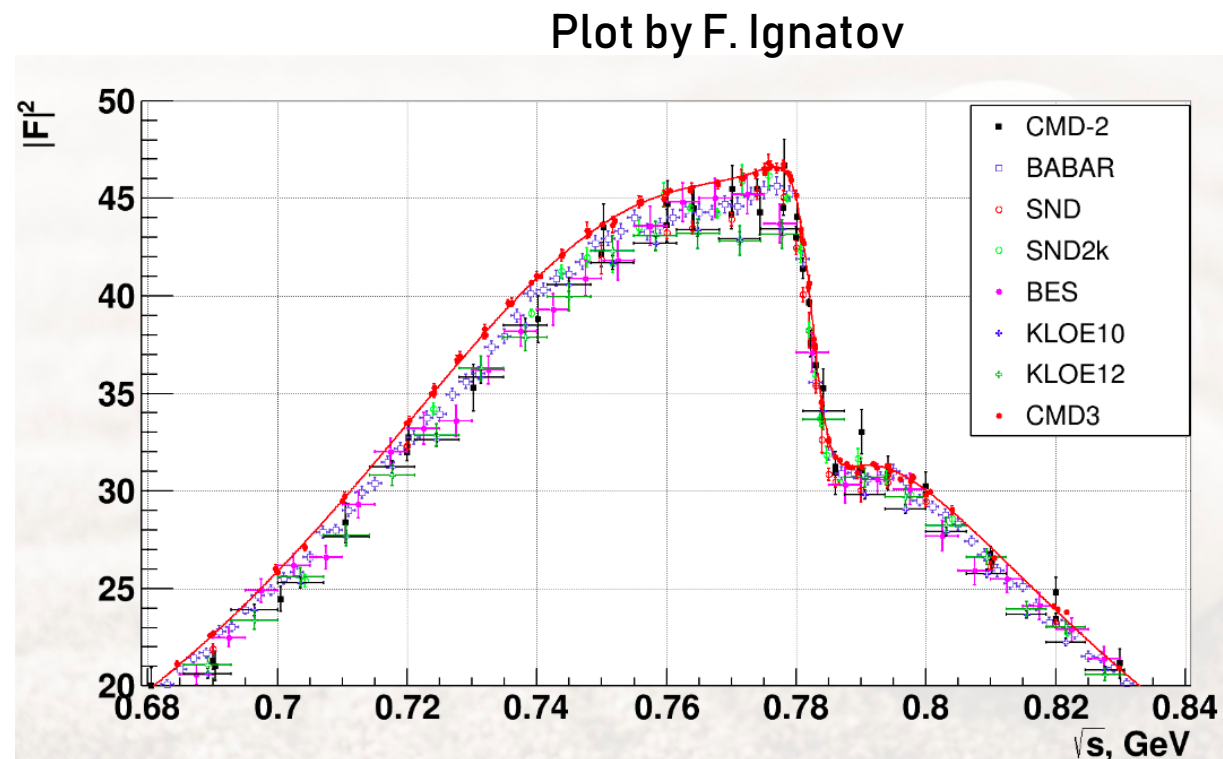
- Tension between dispersive and lattice approaches to HVP
- Lattice result needs independent confirmation
- Long-standing tension between experiment and dispersive result approaches 5σ
- New cross-section results from CMD-3 makes the dispersive situation quite puzzling
- Very dynamic situation: huge effort to reconcile differences and tensions



The CMD-3 result



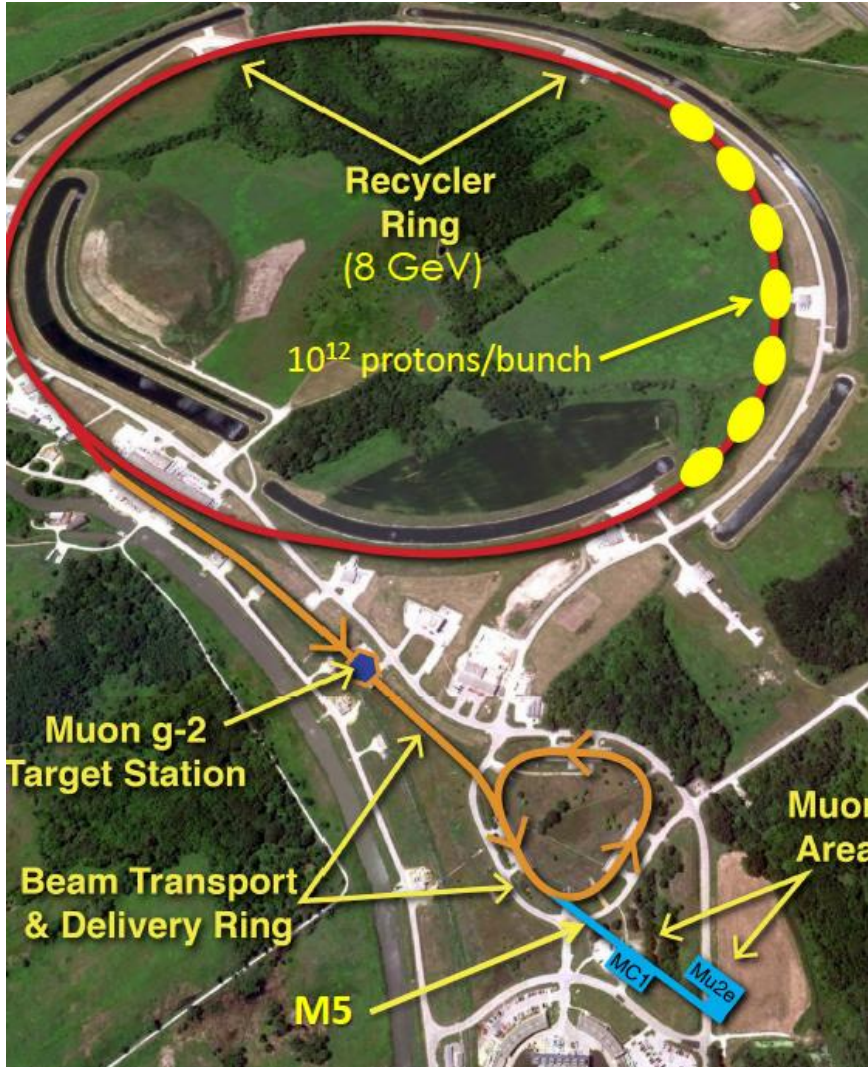
2 new HVP LO results
since WP2020



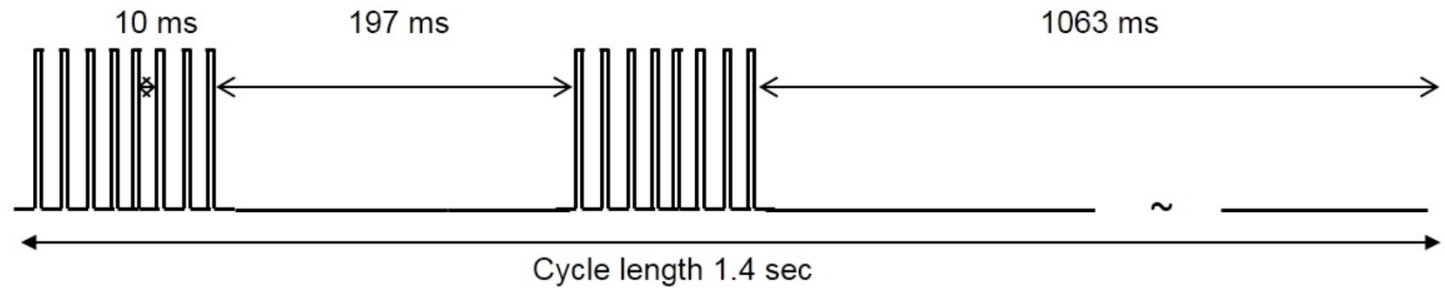
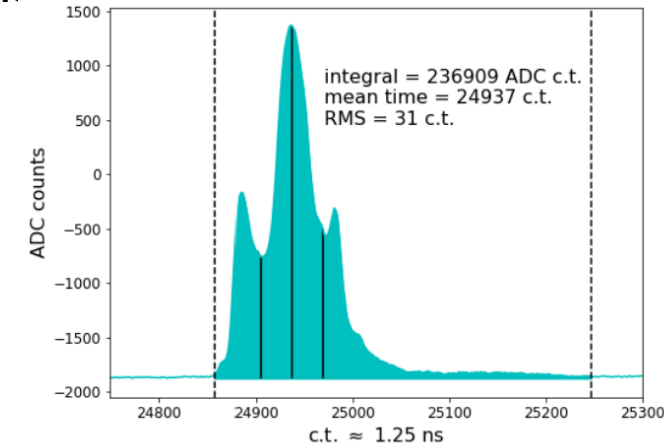
- **SND2k** and **CMD-3** released 2 new results for $a_{\mu}^{\pi^+\pi^-}$ since the theory combination in 2020
- Detailed view of $e^+e^- \rightarrow \pi^+\pi^-$ shows **CMD-3** as outlier, but it agrees with lattice

The Fermilab $g-2$ Experiment

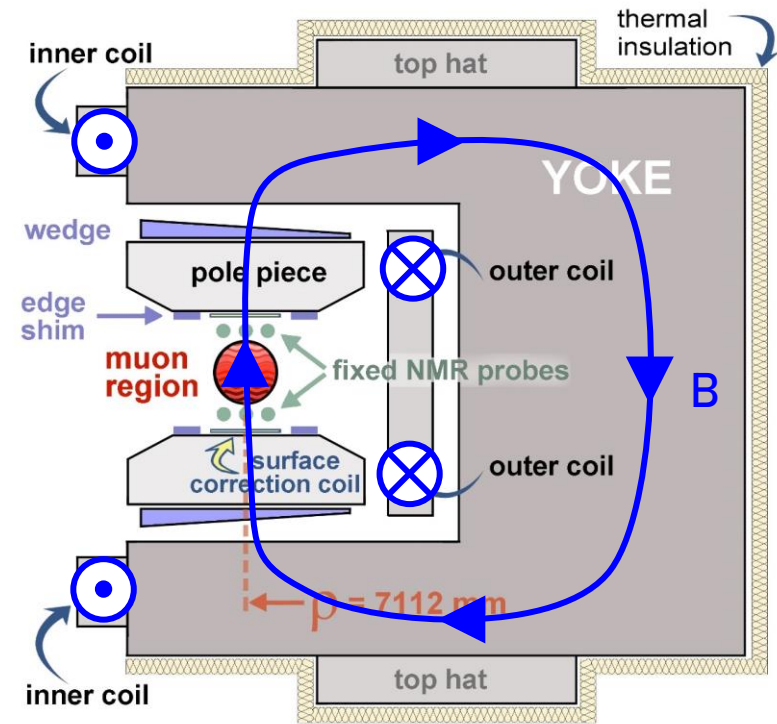
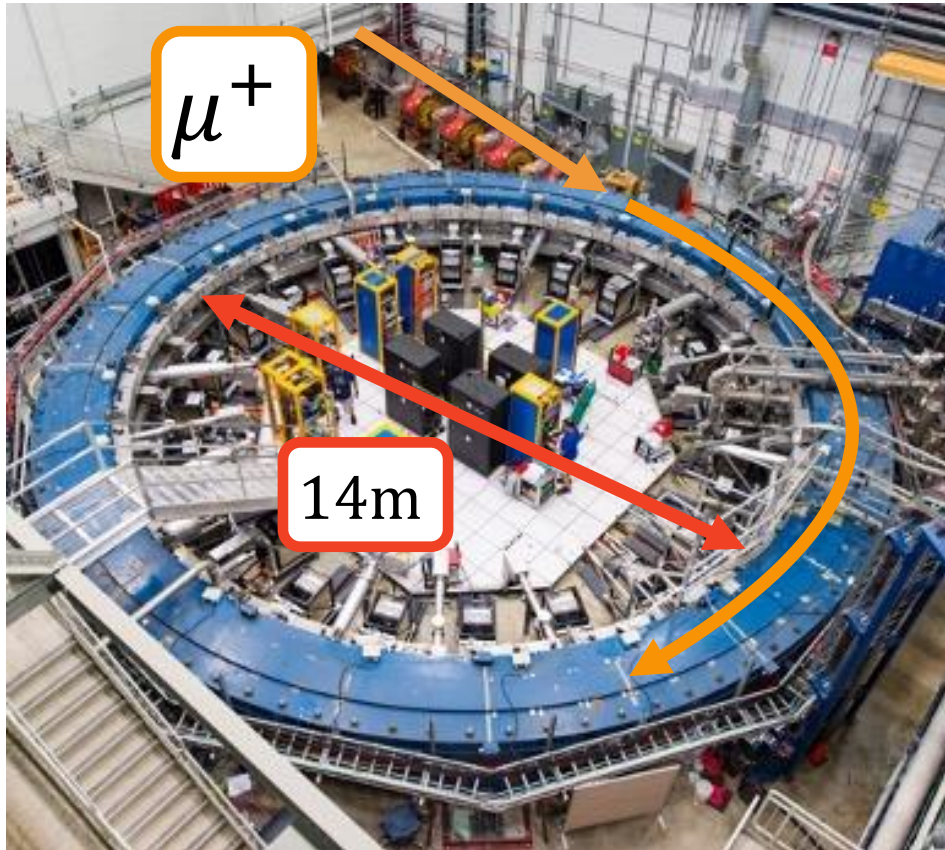
The FNAL Muon Campus



- Recycler ring: 8 GeV protons
 - 10^{12} protons / bunch ; 10k stored muons / bunch
- 8 GeV protons \rightarrow pion production target
- Pions \rightarrow delivery ring \rightarrow decay to μ^+ and momentum-selected
- 3.09 GeV μ^+ \rightarrow g-2 storage ring magnet
- Beam arrives in 120 ns wide bunches
- Each bunch corresponds to a “fill” \rightarrow 1 ms



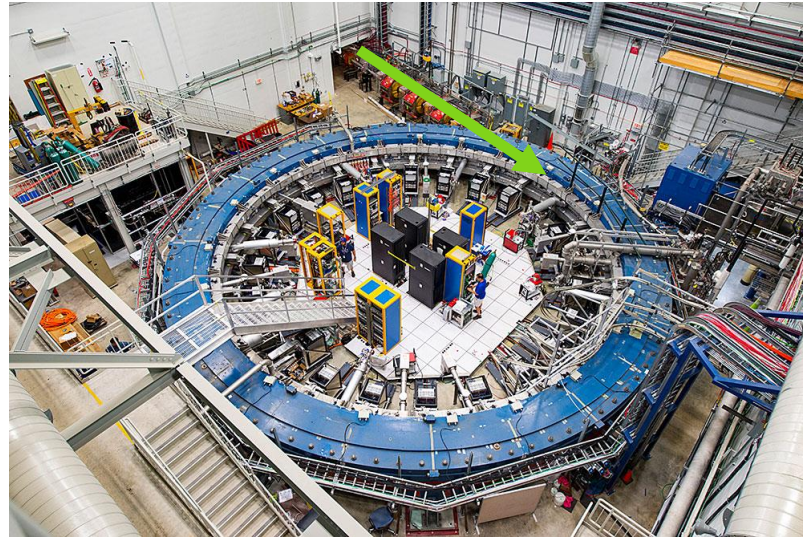
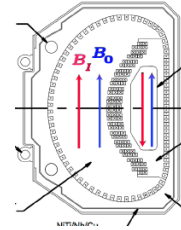
The Storage Ring



Cross-section slice of magnet
1.45 T vertical B field in muon region

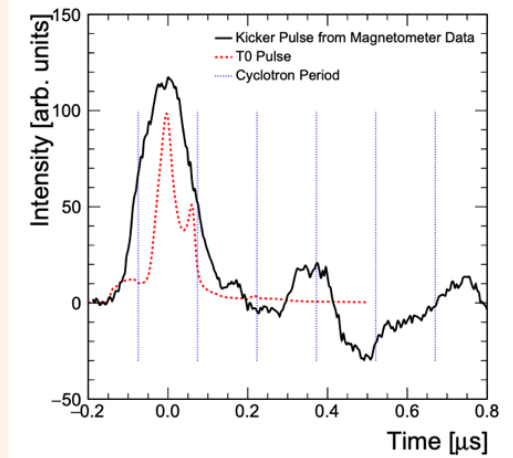
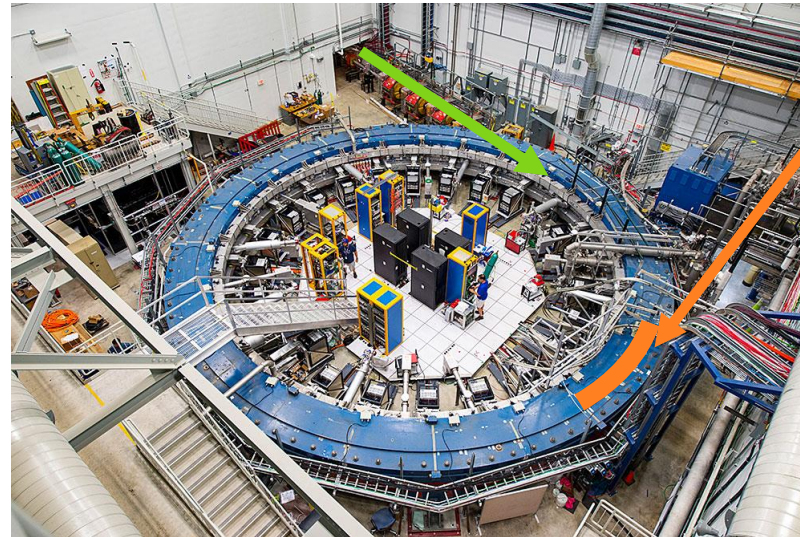
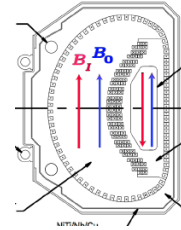
Injecting and storing the beam

Beam injected through
inflexor magnet \rightarrow cancel
main magnetic field



Injecting and storing the beam

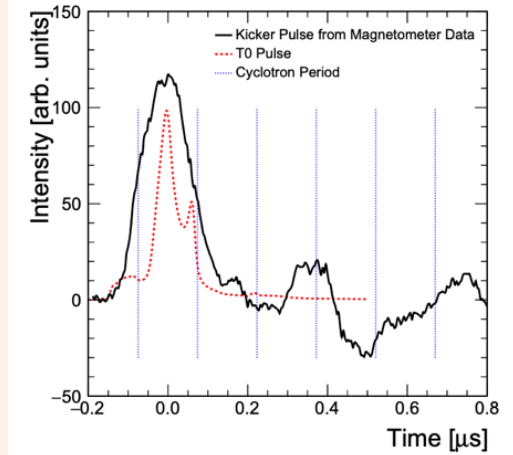
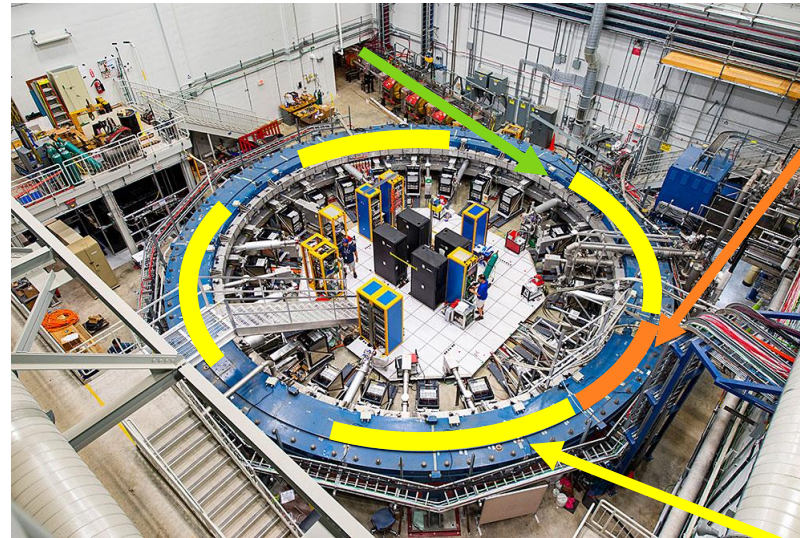
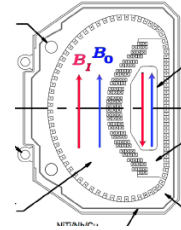
Beam injected through inflector magnet → cancel main magnetic field



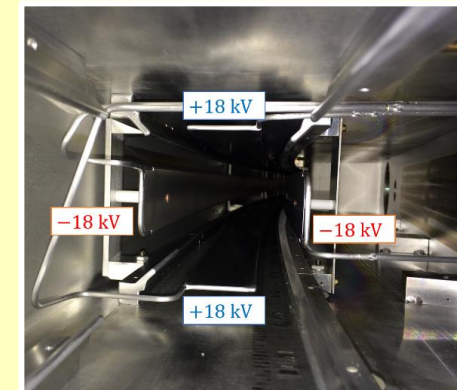
Kicker magnet applies fast radial magnetic field on first turn

Injecting and storing the beam

Beam injected through inflector magnet → cancel main magnetic field



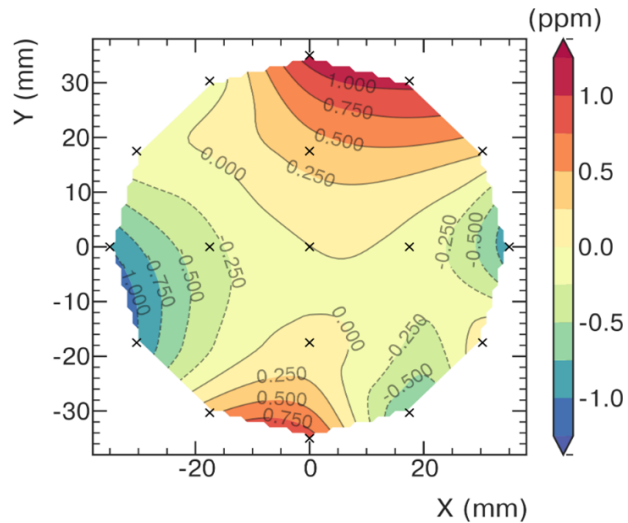
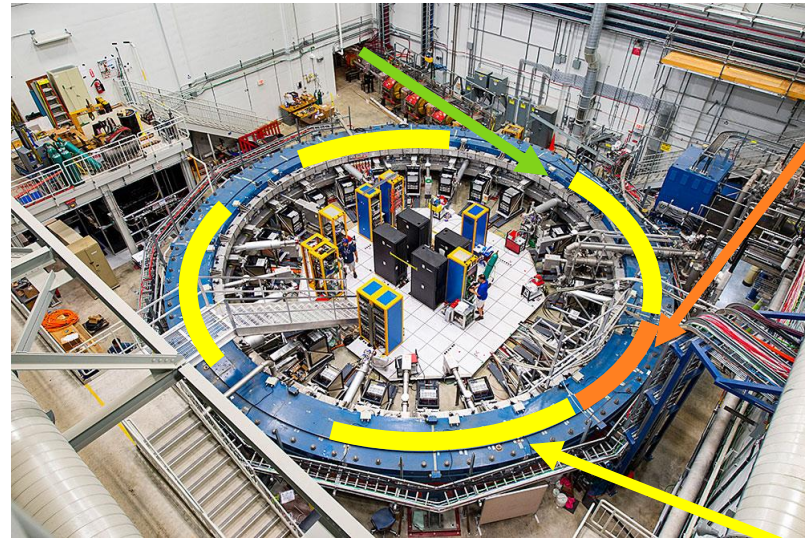
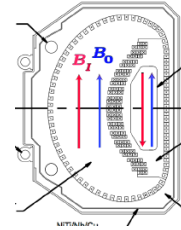
Kicker magnet applies fast radial magnetic field on first turn



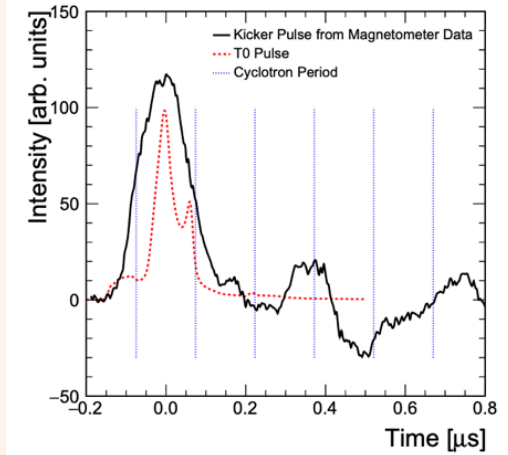
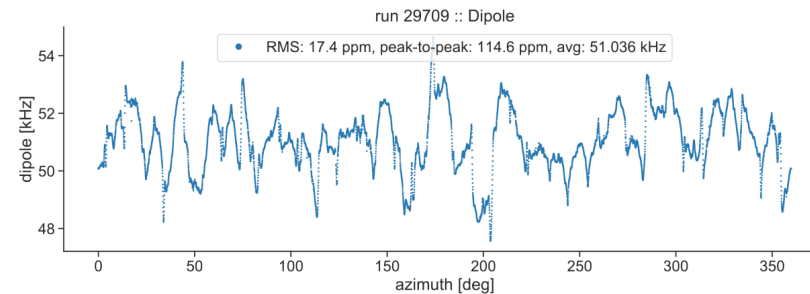
Quads pulse throughout muon fill → vertical focusing

Injecting and storing the beam

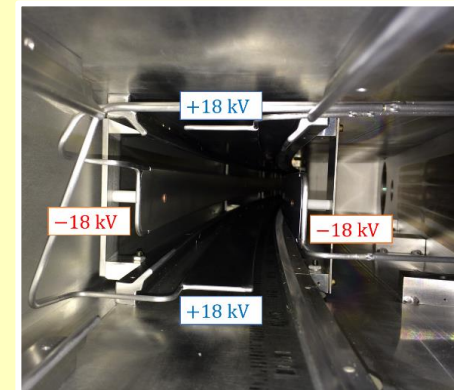
Beam injected through inflector magnet → cancel main magnetic field



Magnetic field map measured every 3 days, changes monitored continuously



Kicker magnet applies fast radial magnetic field on first turn

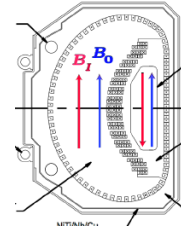


Quads pulse throughout muon fill → vertical focusing

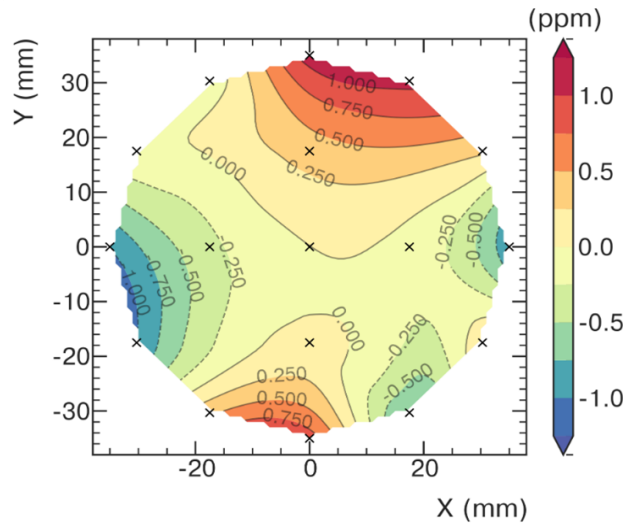
Injecting and storing the beam



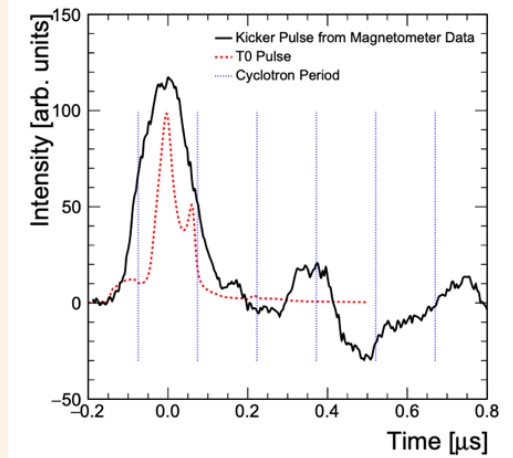
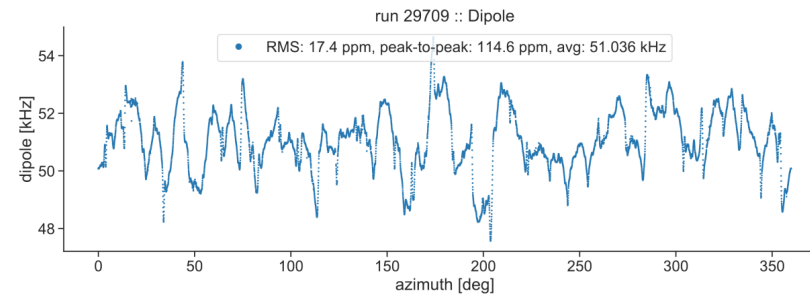
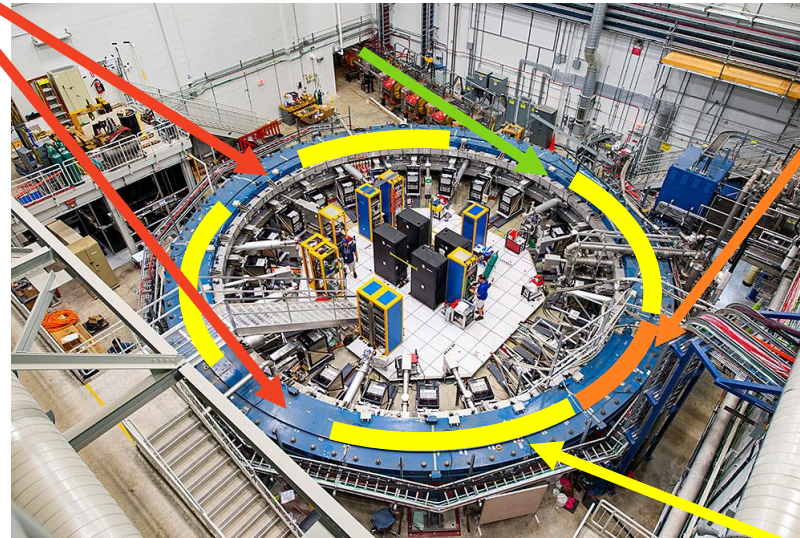
Beam injected through inflector magnet → cancel main magnetic field



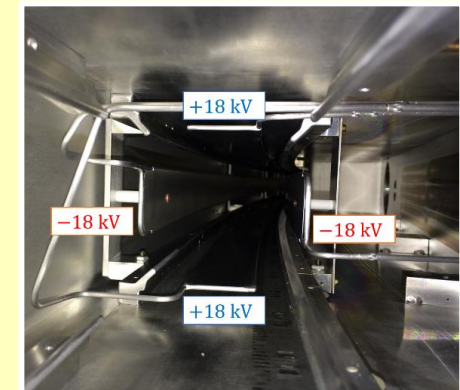
Straw trackers measure beam profile at 180° and 270°



Magnetic field map measured every 3 days, changes monitored continuously



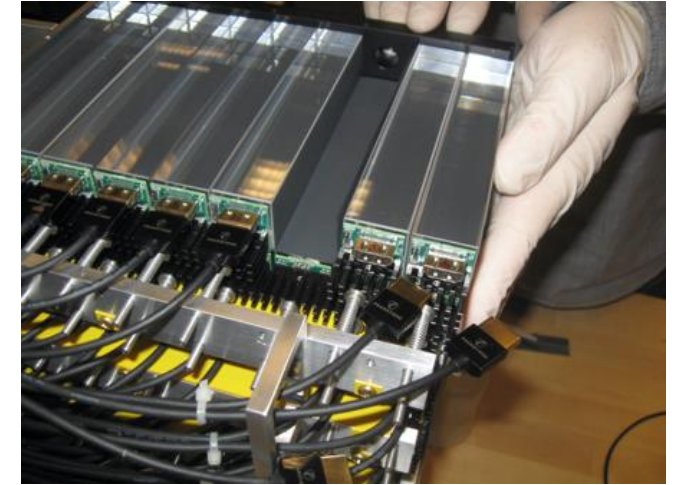
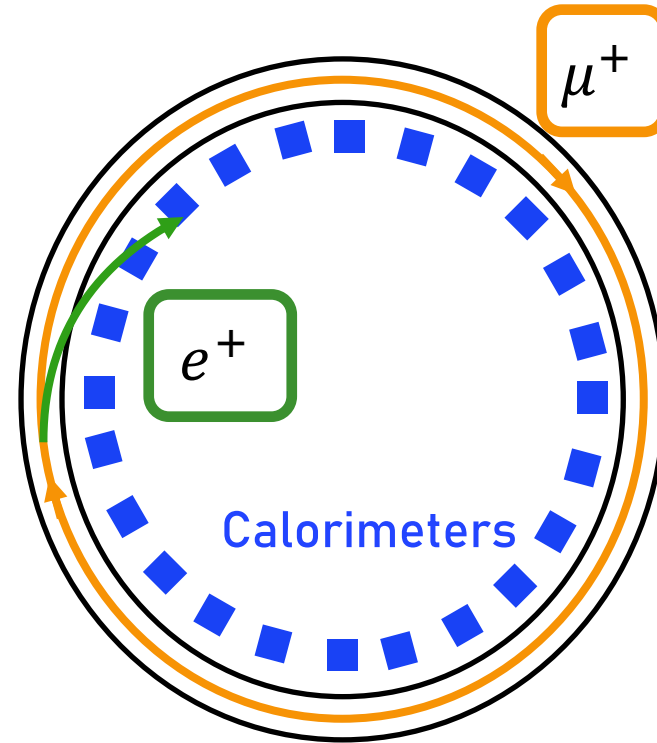
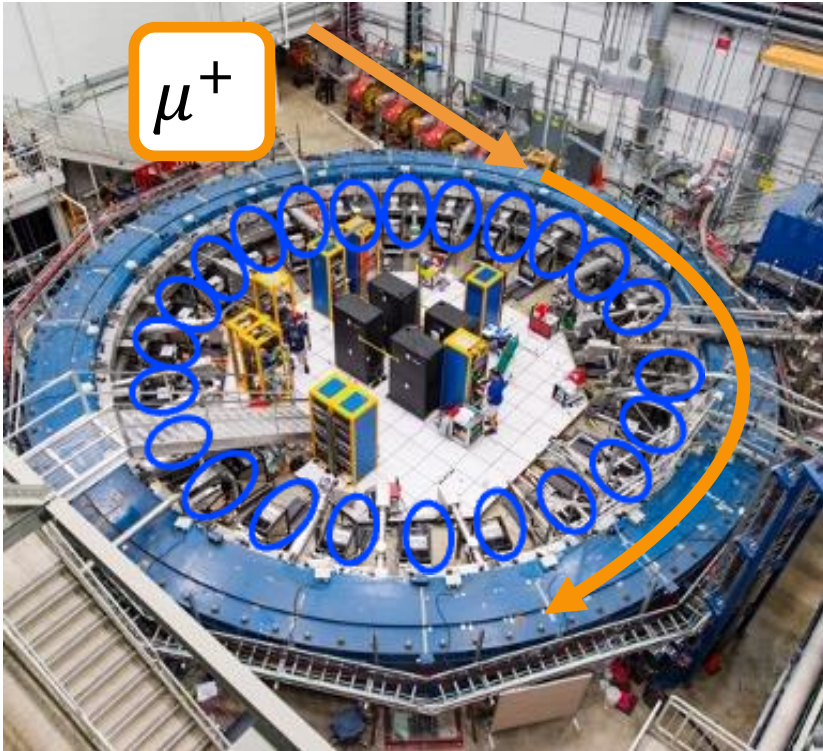
Kicker magnet applies fast radial magnetic field on first turn



Quads pulse throughout muon fill → vertical focusing

Calorimeter detectors

- Positive muons, 3.09 GeV/c, injected into Storage Ring in 125 ns bunches
- Muons orbit inside storage ring, spin precesses about vertical B field
- Decay to positrons \rightarrow lower momentum \rightarrow spiral into centre of storage ring



- Each calo is a 6x9 array of PbF_2 crystals
 - 2.5 cm x 2.5 cm x 14 cm ($15X_0$)
- Readout by SiPMs to 800 MHz WFDs (1296 channels in total)

Spin Precession in the Storage Ring

- Muons orbit the ring with cyclotron frequency ω_c
- Spin precesses with frequency ω_s
- Both **spin** and **cyclotron** frequencies are proportional to **B**
- Spin rotates ahead of momentum as the muon orbits the ring
- **Difference frequency** ω_a is proportional to a_μ and B

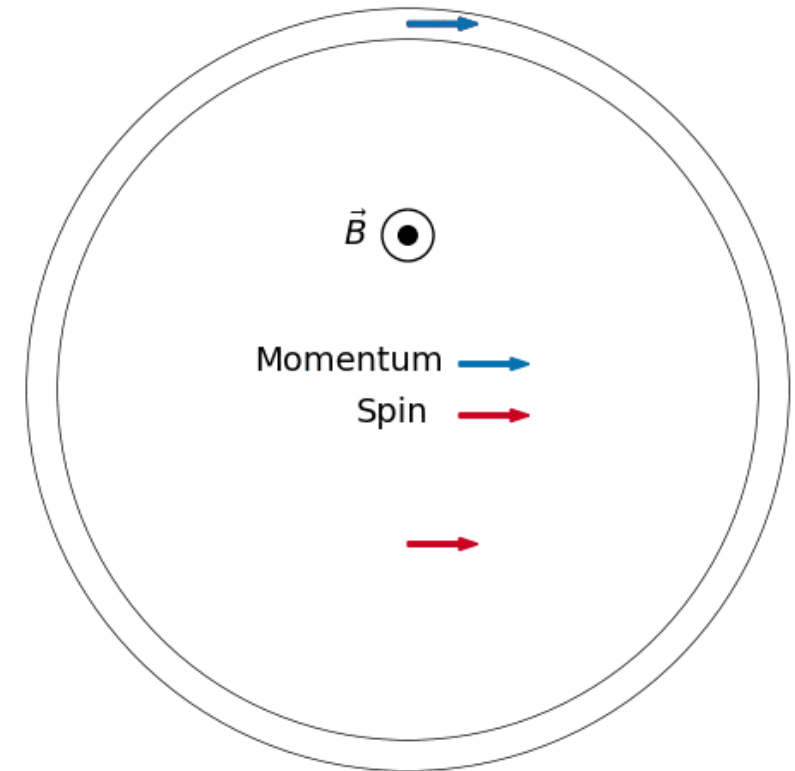
$$\omega_a = \omega_s - \omega_c = a_\mu \frac{eB}{mc}$$

Measure

138 ns

149 ns

Extract



- If g were exactly 2, $\omega_s = \omega_c$ and $\omega_a = 0$

Spin Precession in the Storage Ring

- Muons orbit the ring with cyclotron frequency ω_c
- Spin precesses with frequency ω_s
- Both **spin** and **cyclotron** frequencies are proportional to **B**
- Spin rotates ahead of momentum as the muon orbits the ring
- **Difference frequency** ω_a is proportional to a_μ and B

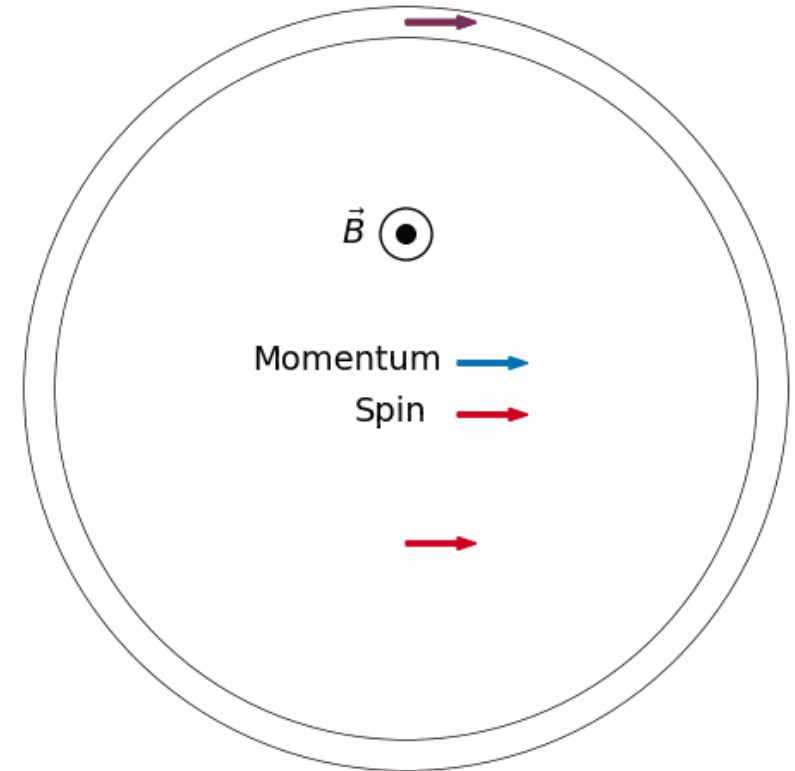
$$\omega_a = \omega_s - \omega_c = a_\mu \frac{eB}{mc}$$

Measure

138 ns

149 ns

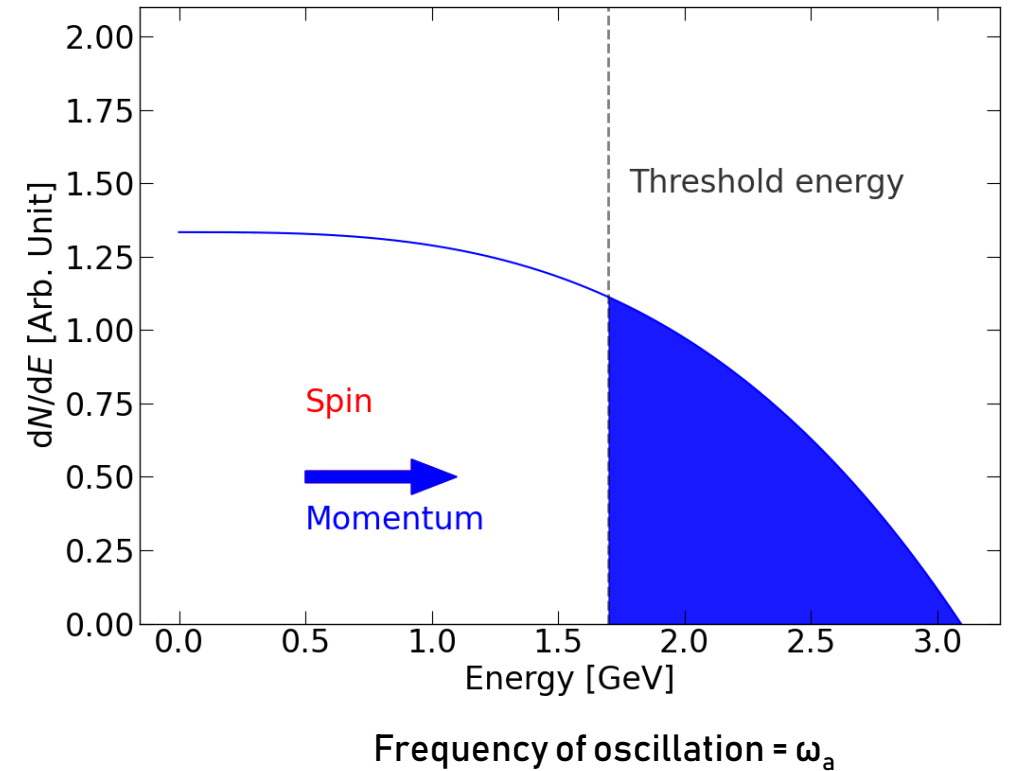
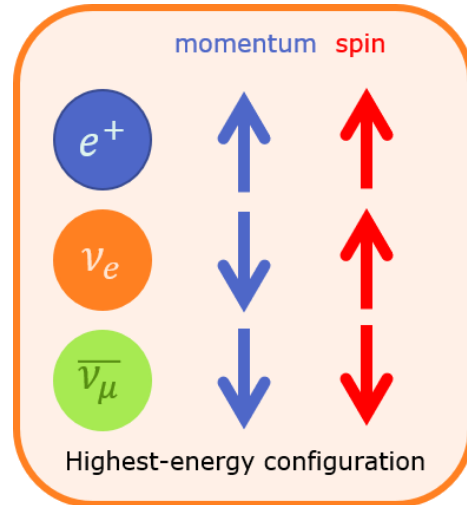
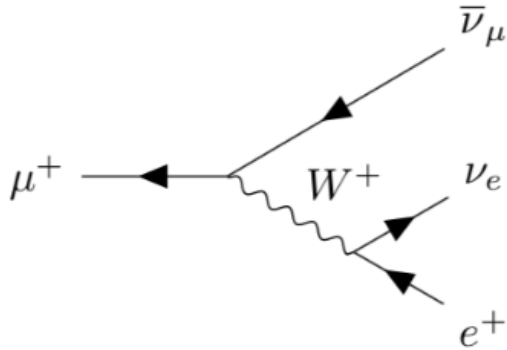
Extract



- If g were exactly 2, $\omega_s = \omega_c$ and $\omega_a = 0$

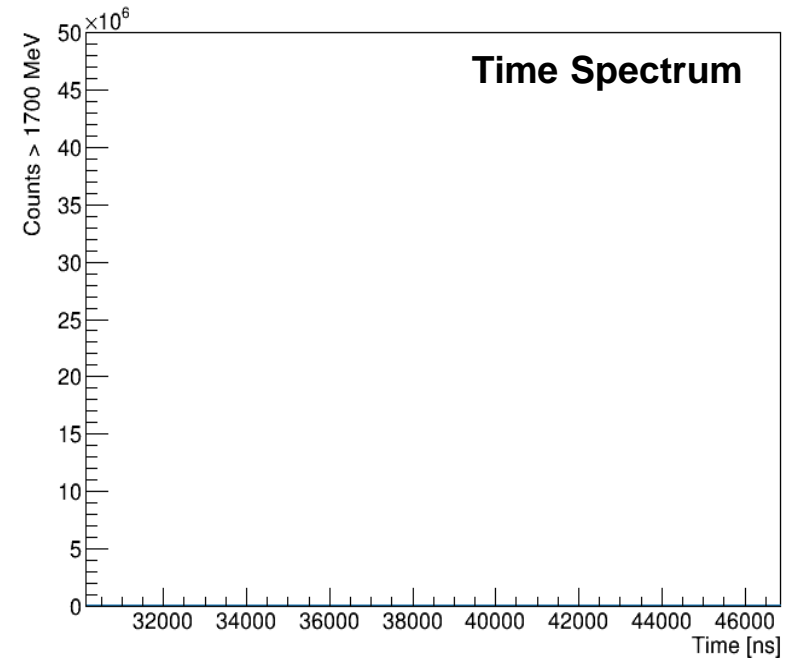
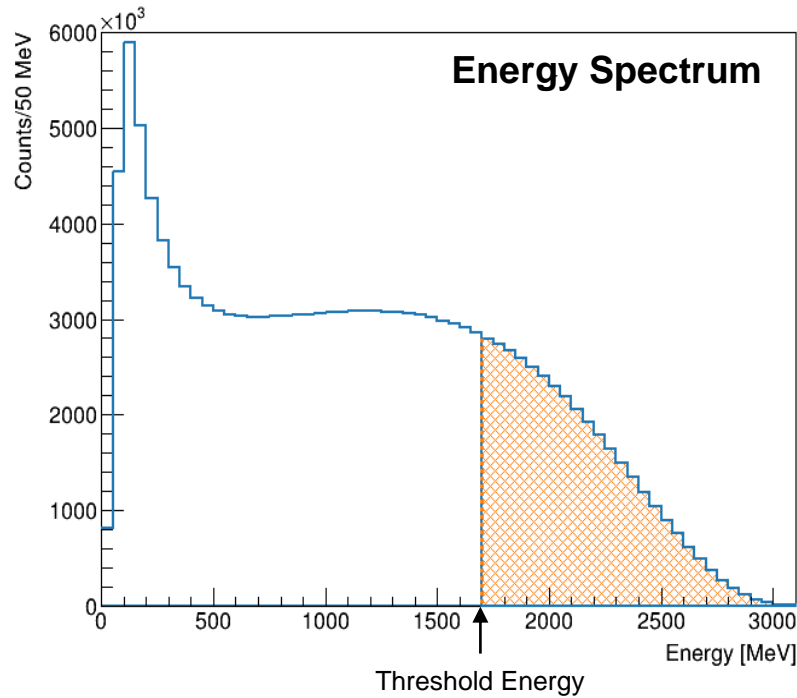
Measuring ω_a

- Highest energy e^+ preferentially emitted in direction of muon spin
- Oscillation in number of emitted decay e^+ vs time directly proportional to decay asymmetry
- Count $N(t)$ = number of e^+ above an energy threshold over time.
- Higher fraction detected above threshold when e^+ emitted parallel to muon spin
- $N(t)$ depends on anomalous precession frequency ω_a



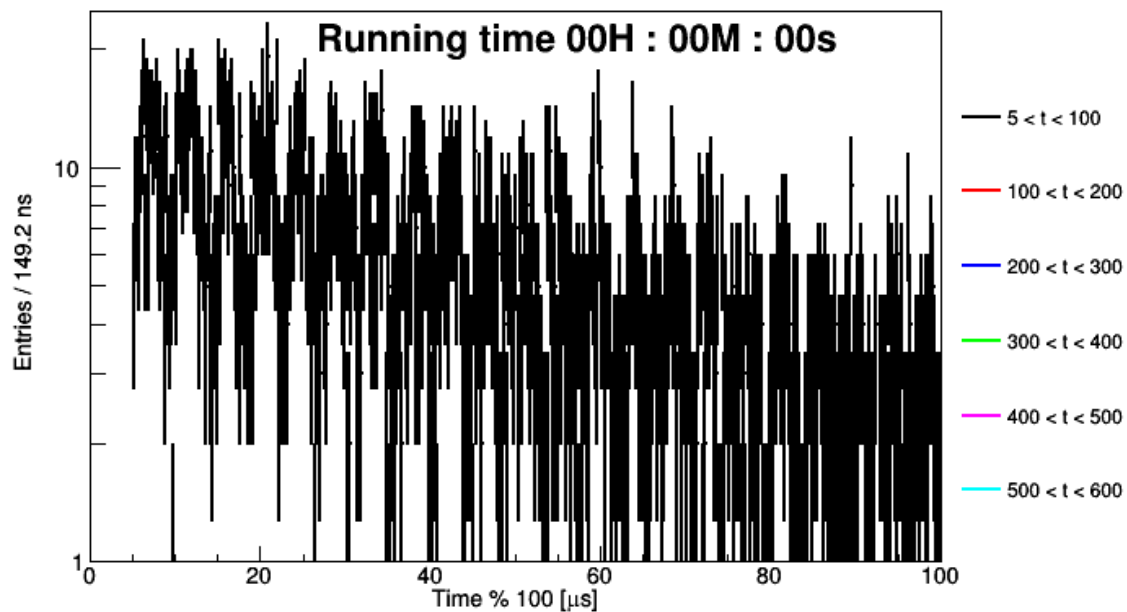
Measuring muon spin precession

- Number of high energy positrons oscillates as a function of time as muon spin points towards/away from detector
- Count positrons above an energy threshold
- Counts oscillate at frequency $\omega_a \rightarrow$ extract from time spectrum



**Real Data
(Run-3a)**

Extracting ω_a : 5-parameter fit function



Five-parameter fit function

$$N(t) = N_0 e^{-t/\tau} [1 - A \cos(\omega_a t + \phi)]$$

Number of e^+ vs time

Time-dilated muon lifetime

Asymmetry

Precession frequency

Average spin phase at injection

Fitting the wiggle

Five-parameter fit function

$$N(t) = N_0 e^{-t/\tau} [1 - A \cos(\omega_a t + \phi)]$$

Number of e^+ vs time

Time-dilated muon lifetime

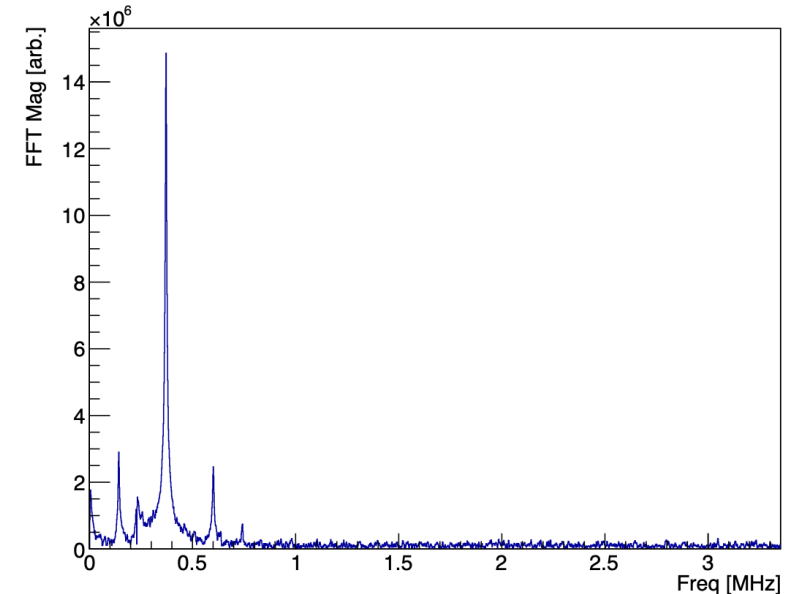
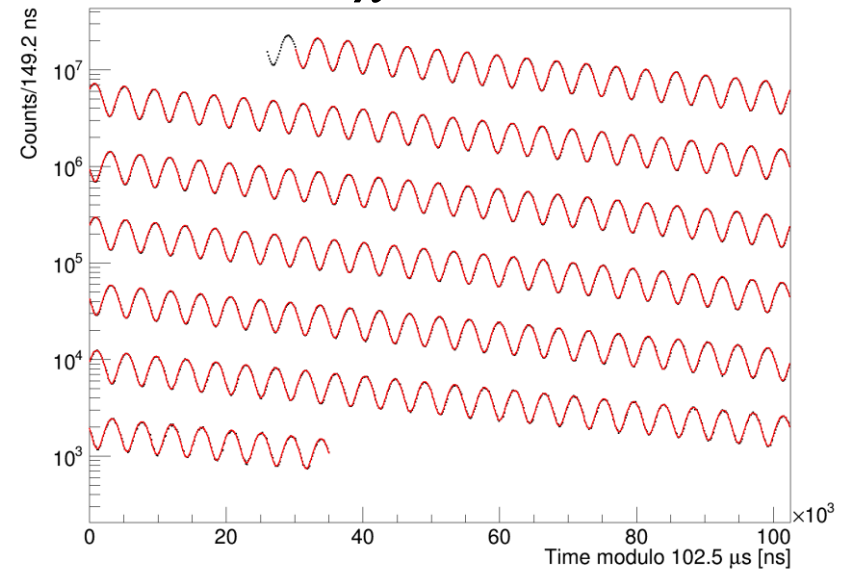
Asymmetry

Precession frequency

Average spin phase at injection

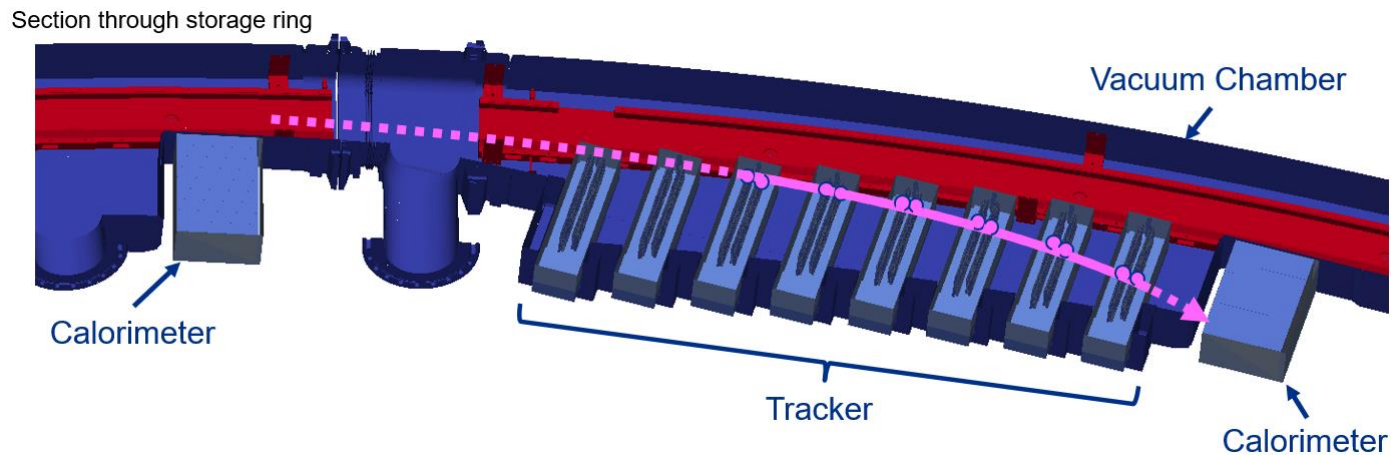
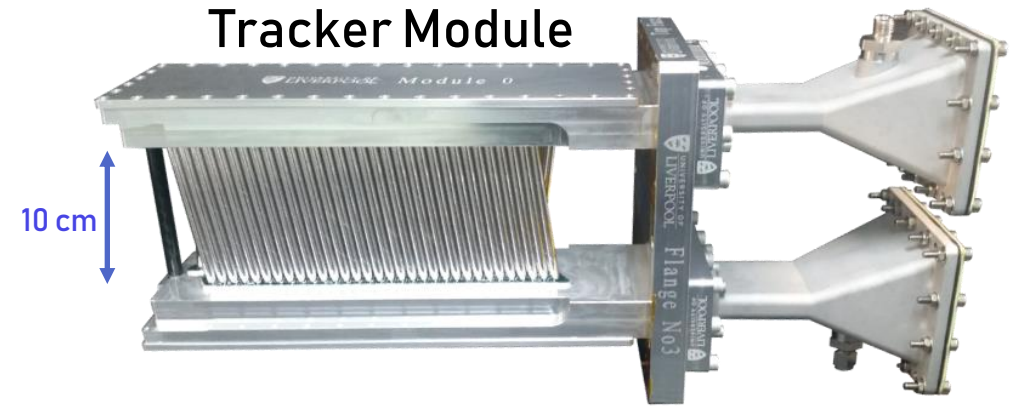
- Simplest 5-parameter fit function captures exponential decay and the g-2 oscillation only
- Not sufficient → large spikes in residuals FFT
- Need to measure and account for additional terms in the fit

$\chi^2/\text{ndf} = 51530/4150$

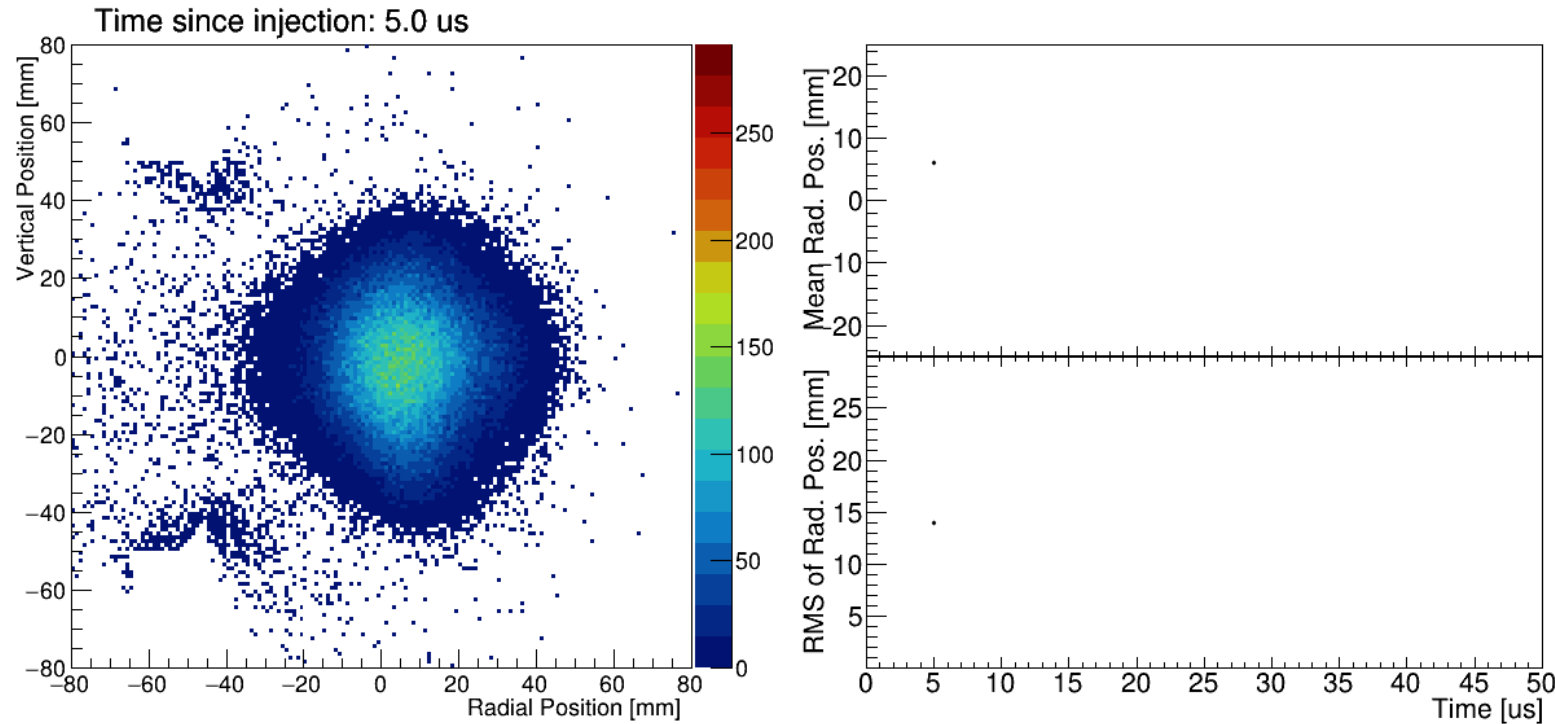


Tracking detectors: measuring the muon beam

- › Straw trackers: two stations located at 180° and 270°
- › One station = 8 modules
- › One module = 128 Argon-Ethane gas-filled straws
- › Fit tracks and extrapolate to muon decay point



Tracker measurement of the muon beam



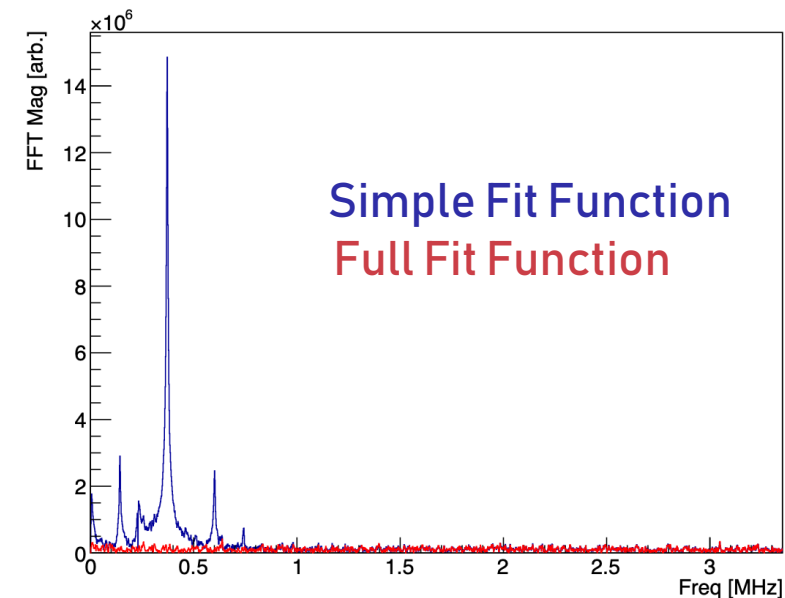
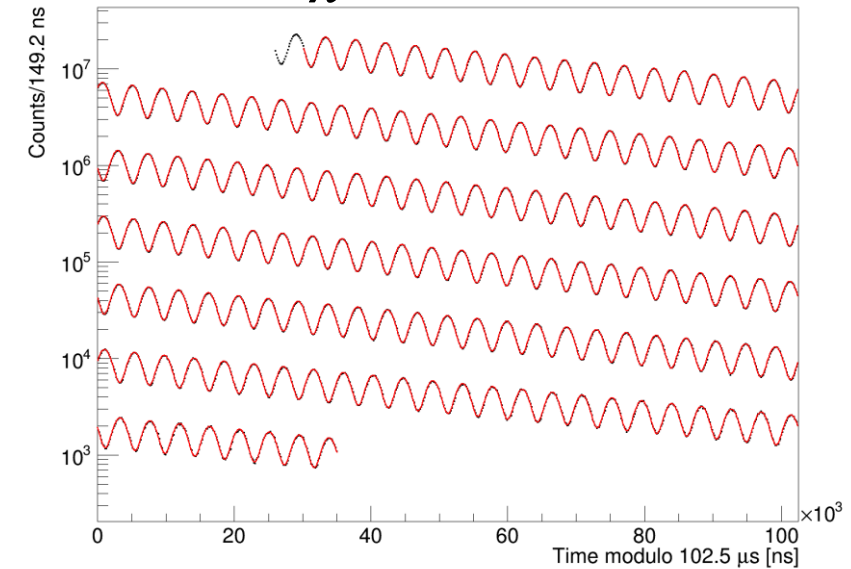
- The mean and width of the muon beam distribution varies as a function of time
- Average radial and vertical position vary around the ring → measure at two locations
- Frequency of beam oscillations must be measured → affects ω_a measurement

Fitting the wiggle

$$\begin{aligned}
 N(t) = & N e^{-t/\tau_\mu} [1 + A \cdot \cos(\omega_a t - \phi + \phi_{BO}(t))] \cdot \\
 & \cdot \left(1 + A_{CBO} \cos(\omega_{CBO} t - \phi_{CBO}) e^{-\frac{t}{\tau_{CBO}}}\right) \cdot \\
 & \cdot \left(1 + A_{VW} \cos(\omega_{VW} t - \phi_{VW}) e^{-\frac{t}{\tau_{VW}}}\right) \cdot \\
 & \cdot \left(1 + A_{2CBO} \cos(\omega_{2CBO} t - \phi_{2CBO}) e^{-\frac{t}{\tau_{2CBO}}}\right) \cdot \\
 & \cdot \left(1 + A_y \cos(\omega_y t - \phi_y) e^{-\frac{t}{\tau_y}}\right) \cdot \\
 & \cdot \left(1 - k_{LM} \int_0^t L(t') e^{t'/\tau_\mu} dt'\right) \cdot \\
 & \cdot \left(1 + [A_+ \cos(\omega_+(t)t - \phi_+) + A_- \cos(\omega_-(t)t - \phi_-)] e^{-\frac{t}{\tau_{CBOVW}}}\right)
 \end{aligned}$$

- Accounting fully for all the beam oscillations shifts ω_a by 1.6 ppm
- Final fit function has 27 fit parameters
- 8 different analysis teams, 19 separate analyses

$\chi^2/ndf = 4086/4138$



Extracting a_μ

Relativistic expression for $\vec{\omega}_a$

$$\vec{\omega}_a = -\frac{q}{m} \left[a_\mu \vec{B} - a_\mu \left(\frac{\gamma}{\gamma + 1} \right) (\vec{\beta} \cdot \vec{B}) \vec{\beta} - \left(a_\mu - \frac{1}{\gamma^2 - 1} \right) \frac{\vec{\beta} \times \vec{\mathcal{E}}}{c} \right]$$

Non-relativistic
limit

Motion non-
perpendicular to B-field

Relativistic motional magnetic field

Proportional to electric field

Cyclotron motion
assumes motion
perpendicular to B-field

Disappears for “magic” $\gamma = 29.3$
→ magic momentum 3.09 GeV / c

Not all muons are at the ‘magic’ momentum of 3.1 GeV

Vertical momentum component aligned with B field

E-field
correction

$$C_E = \frac{\Delta\omega_a}{\omega_a}$$

Pitch
correction

$$C_P = \frac{\Delta\omega_a}{\omega_a}$$

“Never measure anything but frequency...”

$$\vec{\omega}_a = -\frac{q}{m} \left[a_\mu \vec{B} - a_\mu \left(\frac{\gamma}{\gamma + 1} \right) (\vec{\beta} \cdot \vec{B}) \vec{\beta} - \left(a_\mu - \frac{1}{\gamma^2 - 1} \right) \frac{\vec{\beta} \times \vec{\mathcal{E}}}{c} \right]$$

$$a_\mu = \left[\frac{\omega_a}{\tilde{\omega}'_p(T_r)} \right] \frac{\mu'_p(T_r)}{\mu_e(H)} \frac{\mu_e(H)}{\mu_e} \frac{m_\mu}{m_e} \frac{g_e}{2}$$

10.5 ppb Exact 22 ppb 0.28 ppt

- We measure the ratio of **two frequencies**: ω_a and ω_p
 - ω_a : anomalous spin precession frequency
 - ω_p : muon-weighted magnetic field expressed in terms of Larmor frequency of free proton

Phys. Rev. A **83**, 052122 (2011)

Metrologia **13**, 179 (1977)

Rev. Mod. Phys. **88** 035009 (2016)

Phys. Rev. Lett. **82**, 711 (1999)

“... and corrections”

$$a_{\mu} \propto \frac{f_{\text{clock}} \omega_a^m (1 + C_e + C_p + C_{ml} + C_{pa})}{f_{\text{calib}} \langle \omega'_p(x, y, \phi) \times M(x, y, \phi) \rangle (1 + B_k + B_q)}$$

Clock blinding frequency

Anomalous precession frequency

Beam dynamics corrections

Absolute calibration frequency

Magnetic field map

Muon beam distribution

Transient magnetic field corrections

“... and corrections”

$$a_{\mu} \propto \frac{f_{\text{clock}} \omega_a^m (1 + C_e + C_p + C_{ml} + C_{pa})}{f_{\text{calib}} \langle \omega'_p(x, y, \phi) \times M(x, y, \phi) \rangle (1 + B_k + B_q)}$$

Absolute calibration frequency

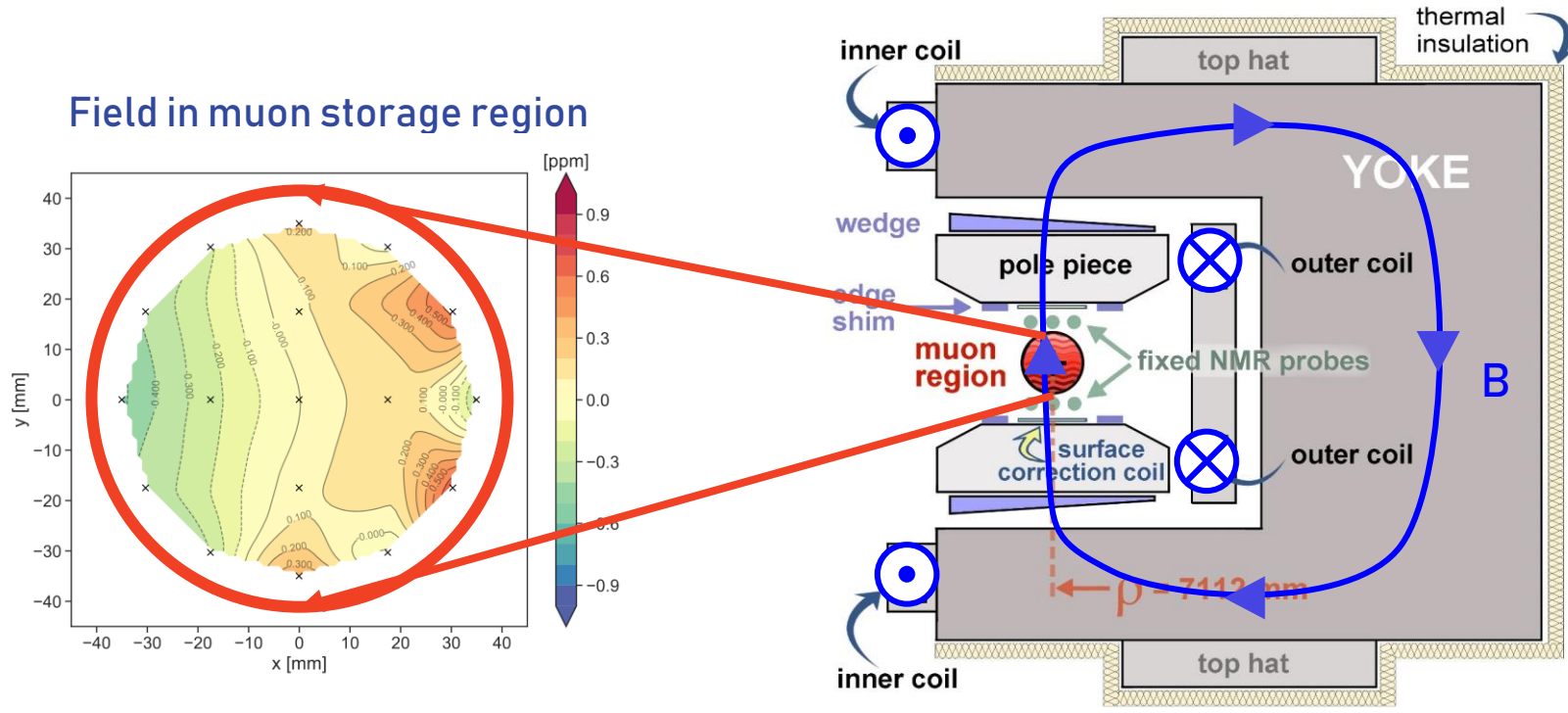
Magnetic field map

Muon beam distribution

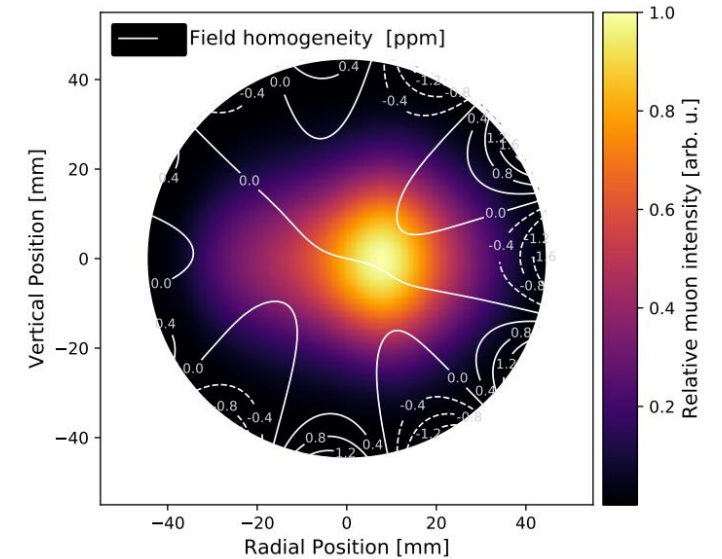
Transient magnetic field corrections

Measuring the magnetic field

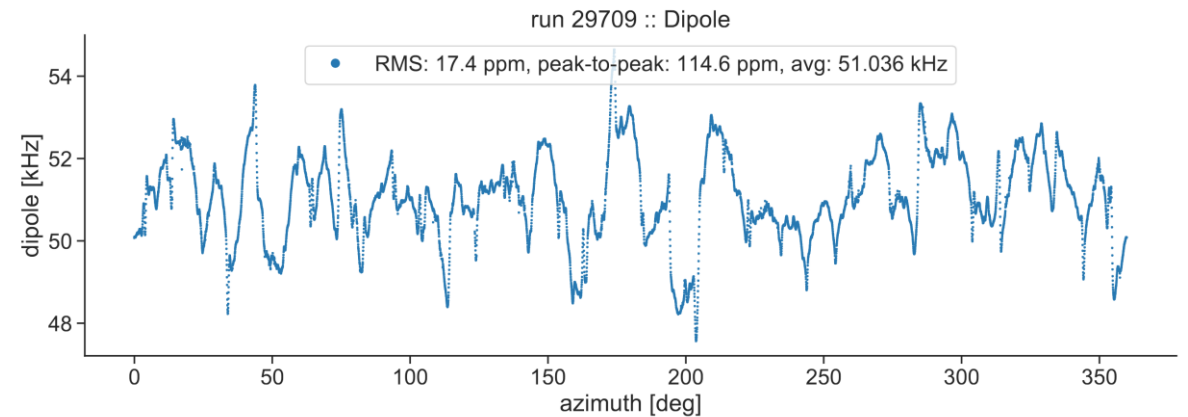
The g-2 Storage Ring magnet



Weight measured field by the muon beam distribution

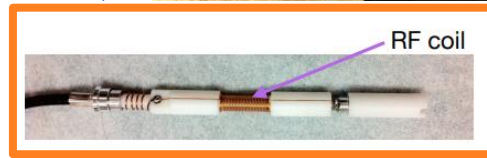
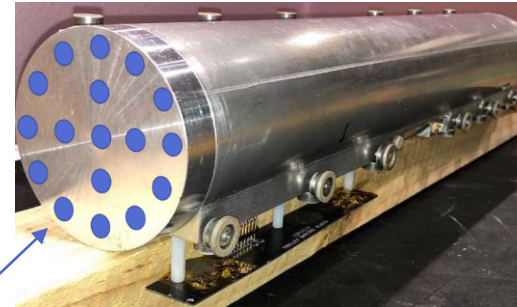


- Dipole field has **ppm-level uniformity** (<20 ppm RMS across the full azimuth)
- **Shimming devices** (active and passive) minimise gradients and keep field uniform

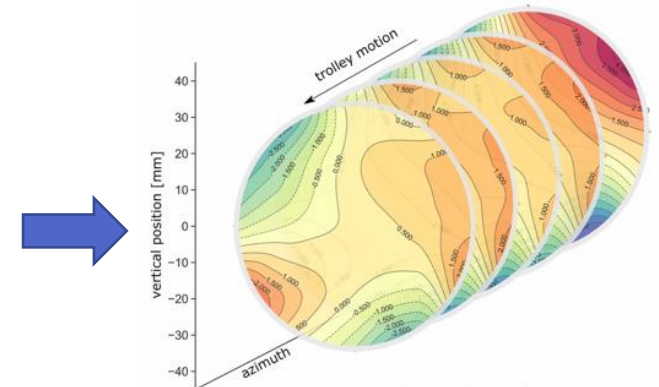


Measuring the magnetic field

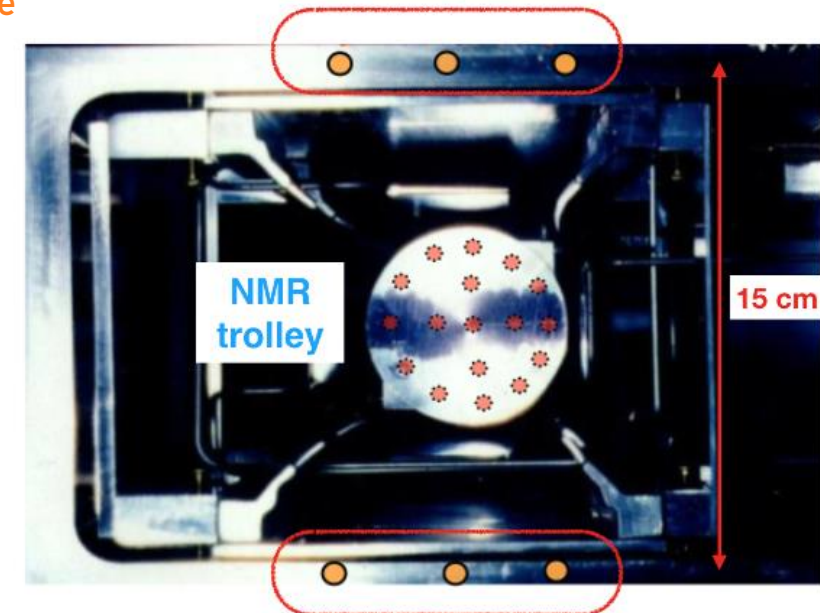
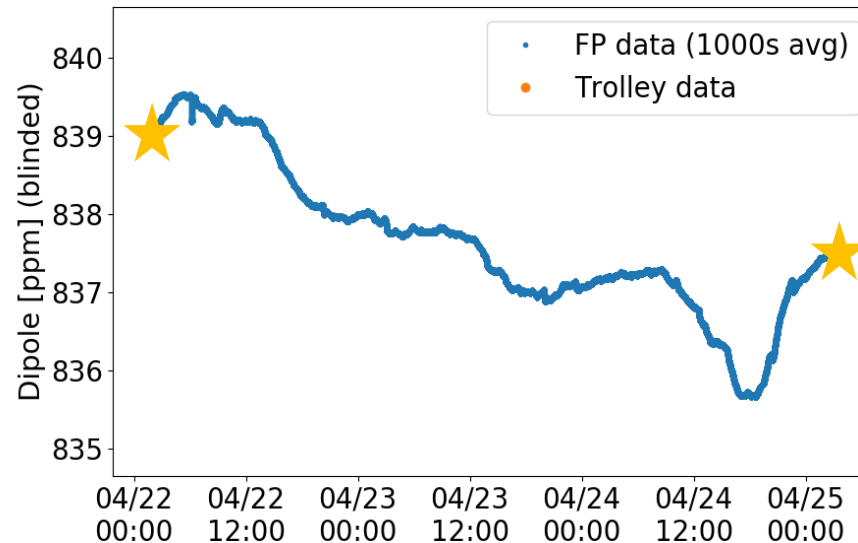
- Trolley containing 17 NMR probes maps full azimuth every few days (muons not present)
- 378 fixed probes monitor between trolley runs (during muon data collection)
- Field map is interpolated between trolley runs using fixed probe information
- Fold with muon beam distribution



NMR probe



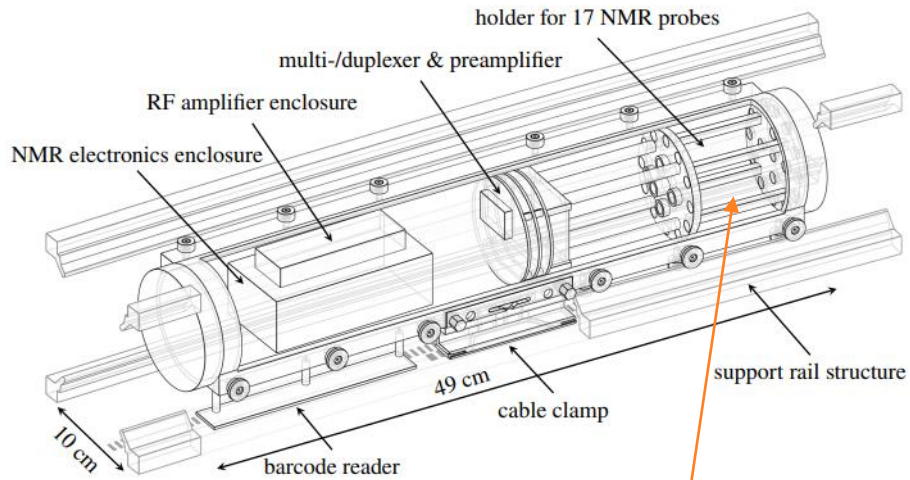
Sequence 2D field slices as trolley moves



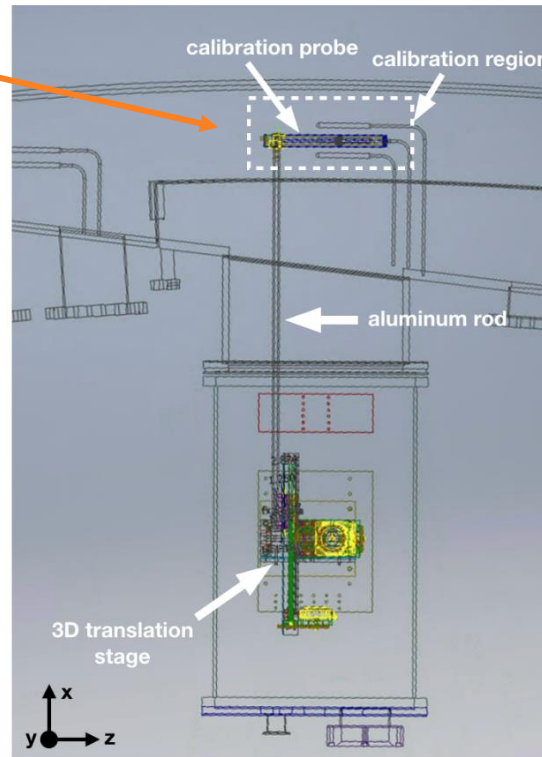
Absolute Calibration

- Trolley and fixed NMR probes use **petroleum jelly** as the proton sample – **low volatility**
- Need to measure **protons in H₂O** (measurement standard) → calibration
- Trolley and **cylindrical H₂O** calibration probe switch places to repeatedly measure the same field in the **same place**. Calibration performed ~once per year.

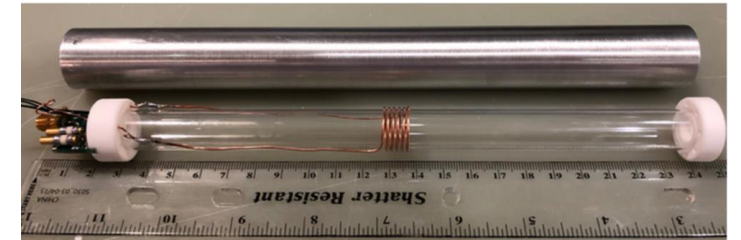
Uncertainty
17 ppb



Calibration region



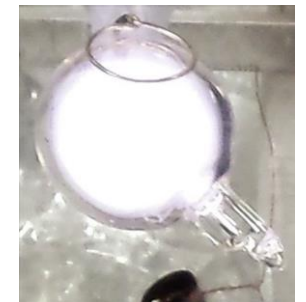
Cylindrical H₂O probe



Spherical H₂O



Spherical ³He

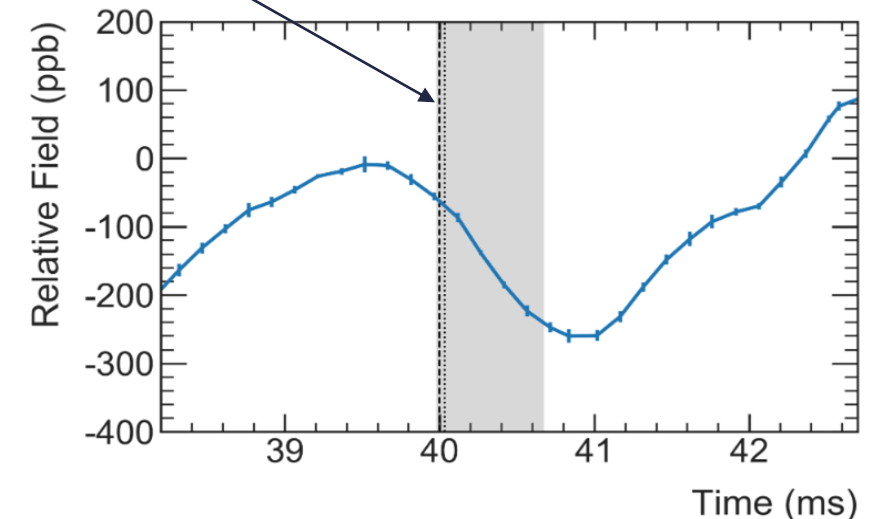
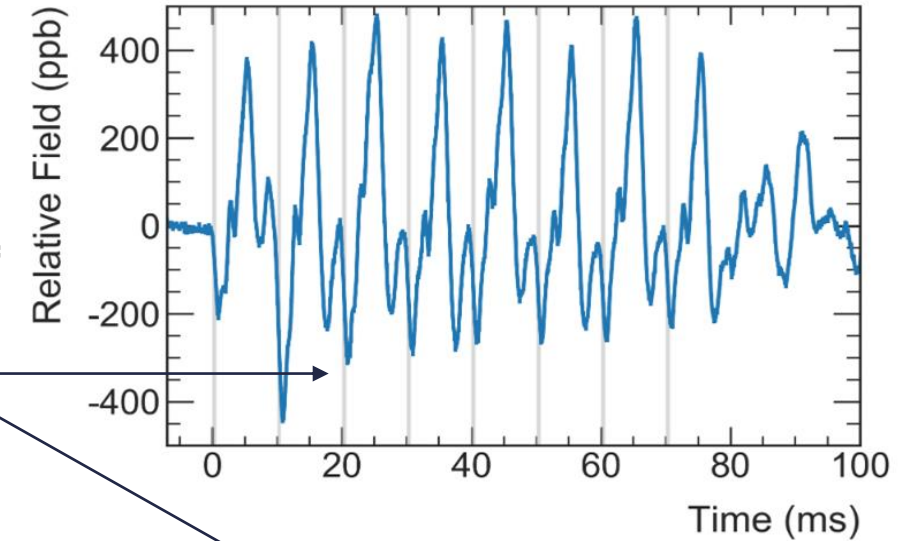
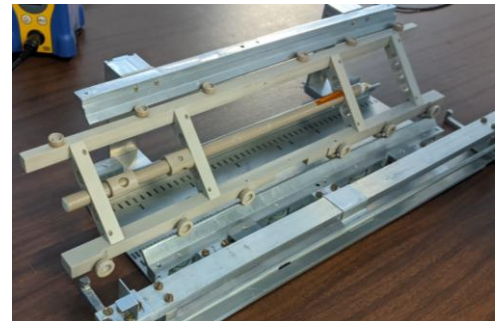
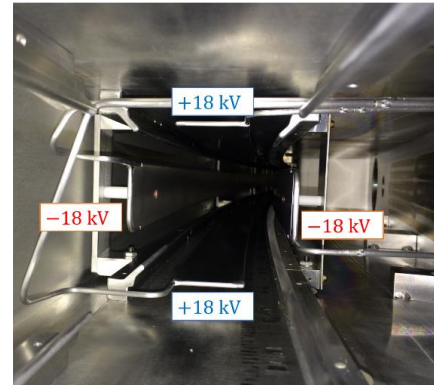
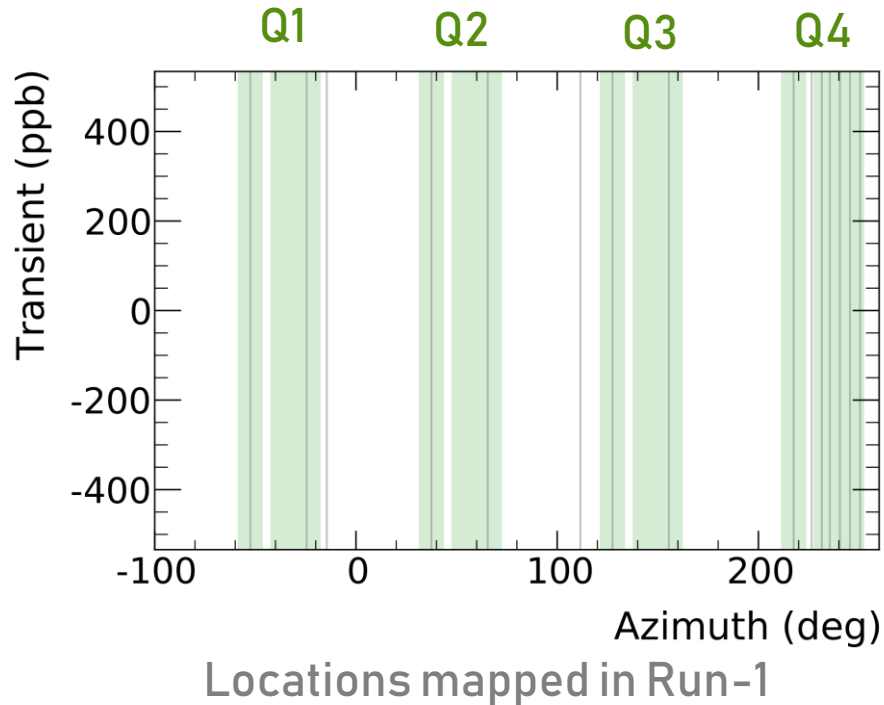


Cross-check with spherical probes
Uncertainty: 9 ppb

Transient fields from pulsed systems: Quads

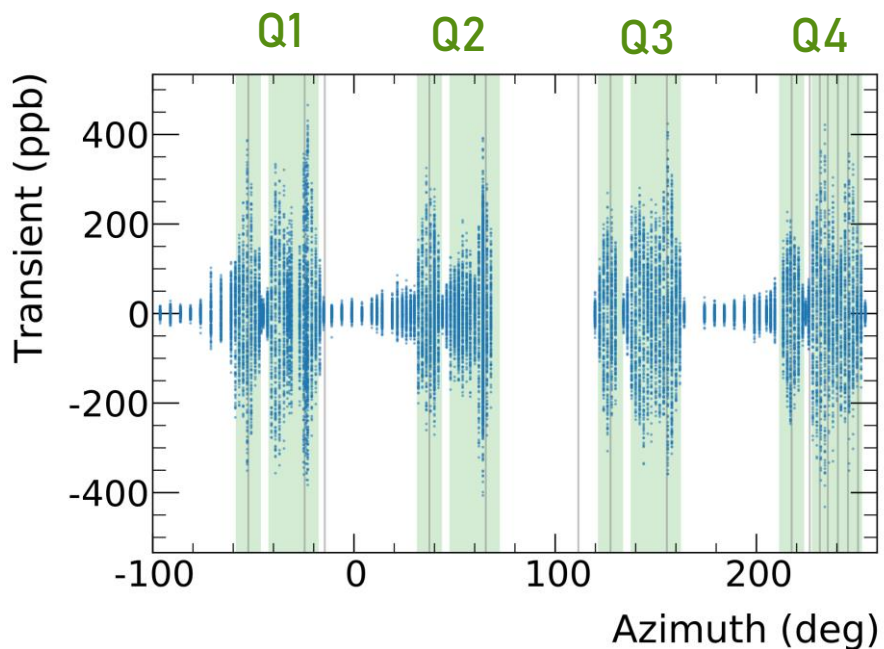
- Electrostatic quadrupoles pulse during muon storage
- No pulsing during trolley runs
- Quad plates vibrate \rightarrow induces a field
- Muons experience a field change which the fixed probes do not see (shielded by Al)
- Must be measured using dedicated apparatus

Grey regions =
muon storage
times

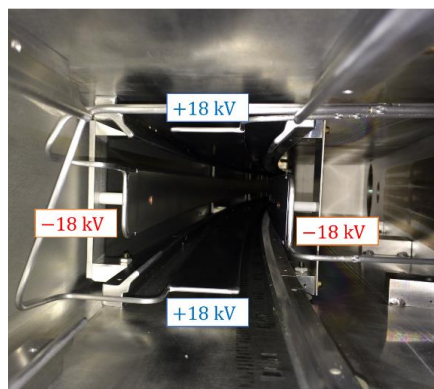


Transient fields from pulsed systems: Quads

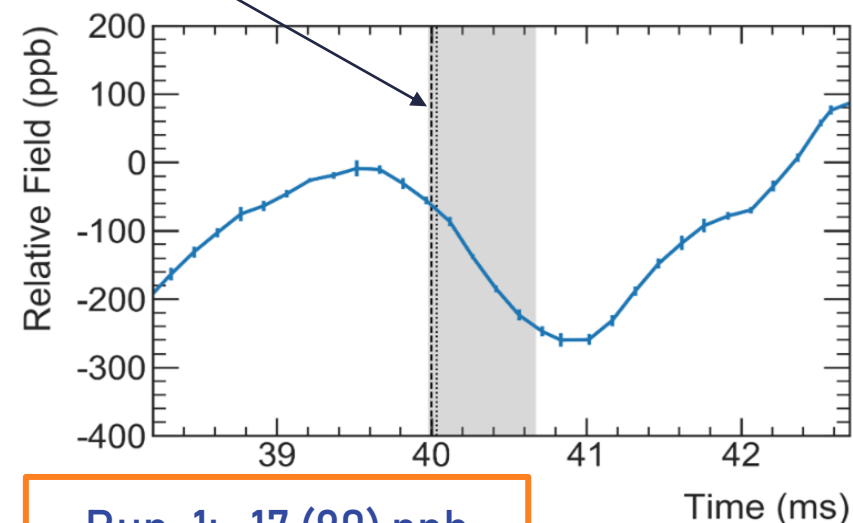
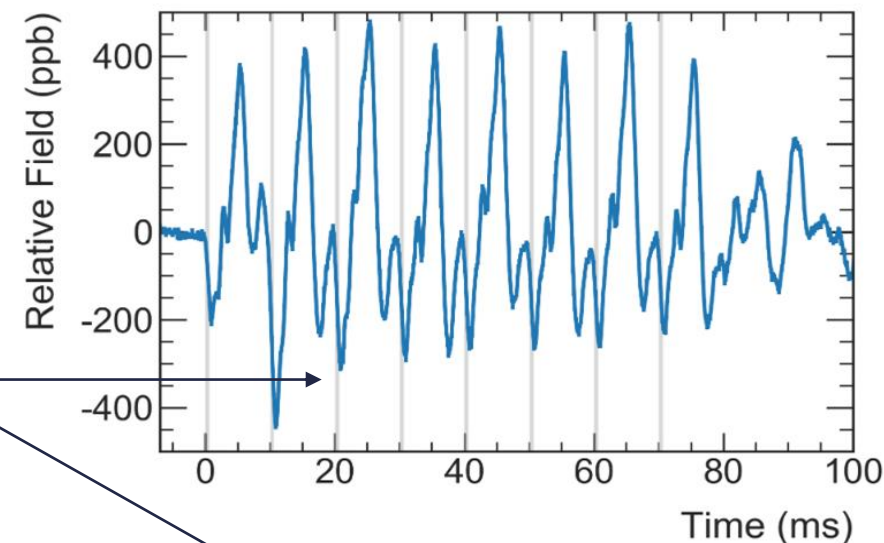
- Electrostatic quadrupoles pulse during muon storage
- No pulsing during trolley runs
- Quad plates vibrate \rightarrow induces a field
- Muons experience a field change which the fixed probes do not see (shielded by Al)
- Must be measured using dedicated apparatus



Locations mapped in Run-2



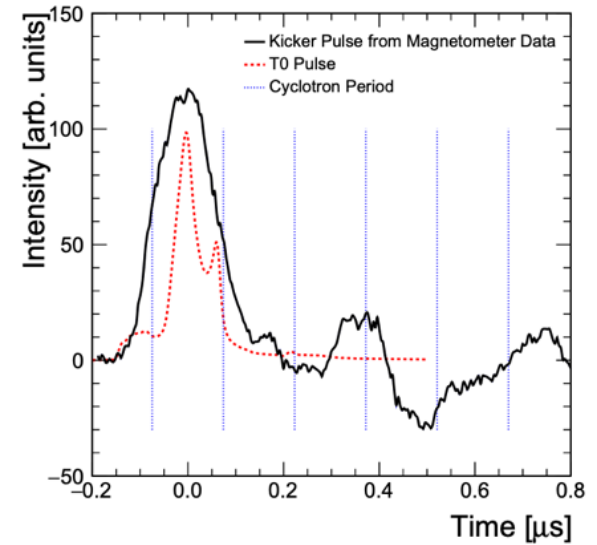
Grey regions =
muon storage
times



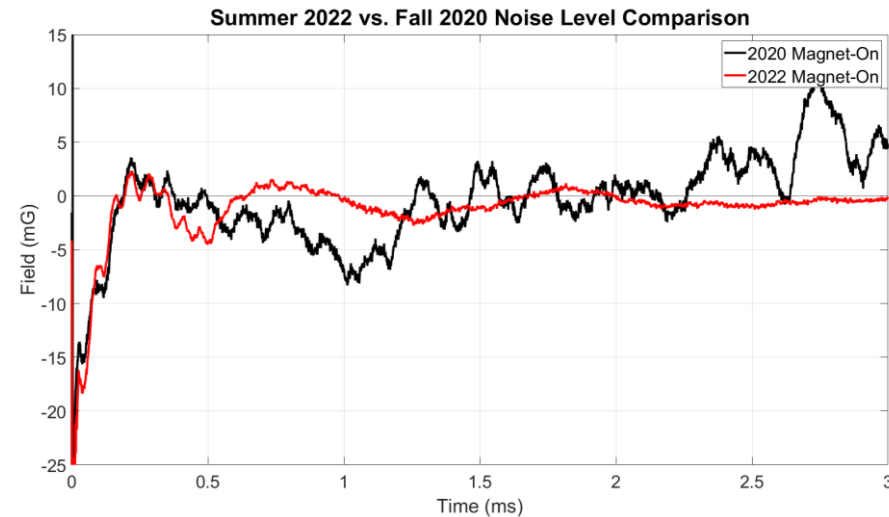
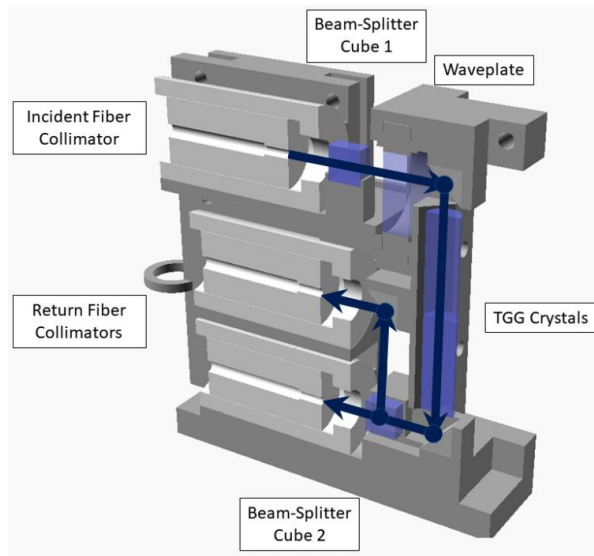
Run-1: -17 (90) ppb
Run-2/3: -21 (20) ppb

Transient fields from pulsed systems: Kicker

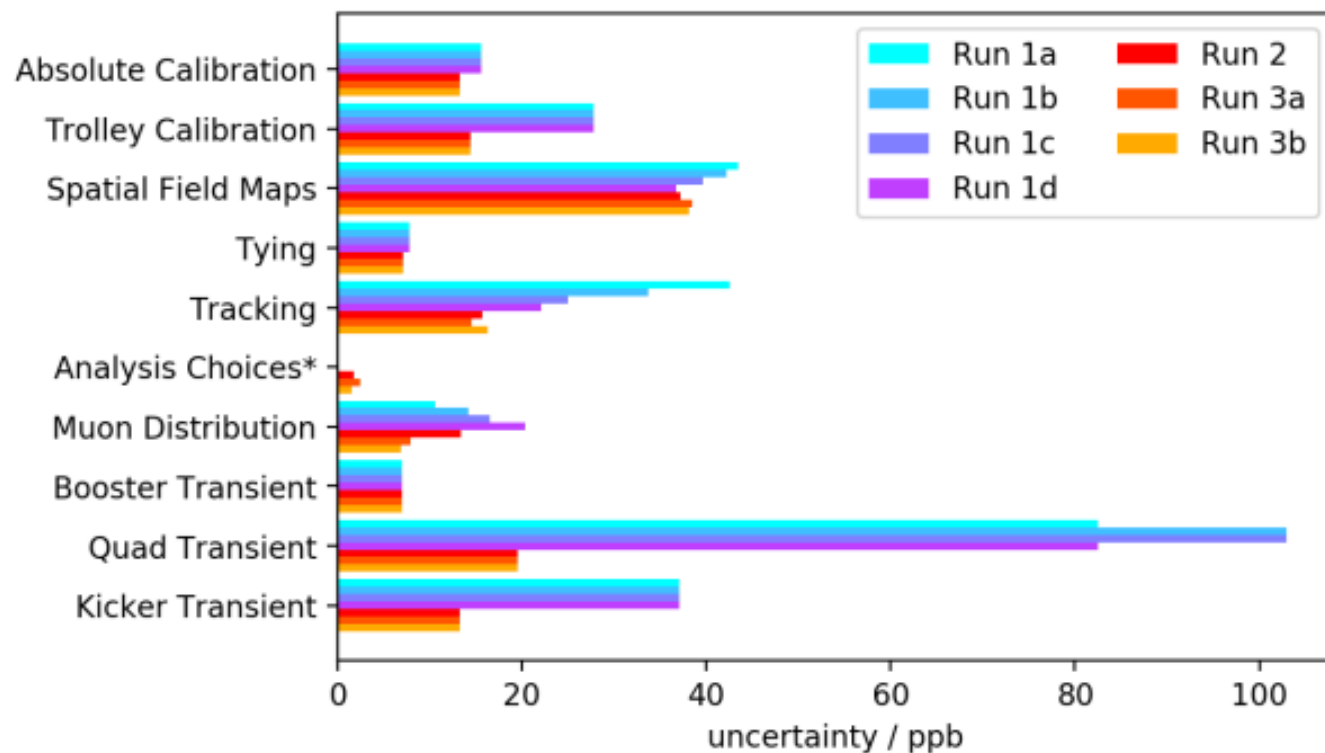
- Kicker pulse of **22 mT for 150 ns** just after muon injection
- Field change caused by residual field (eddy currents) after kicker pulse
- Muons present from **30 μ s to 700 μ s** after the kick (fit region)
- Measure eddy current using Faraday magnetometer
- Run-2/3: improved hardware setup reduced vibrations



Correction
Run-1: -27 (37) ppb
Run-2/3: -21 (13) ppb



Magnetic field systematics in Run-2/3

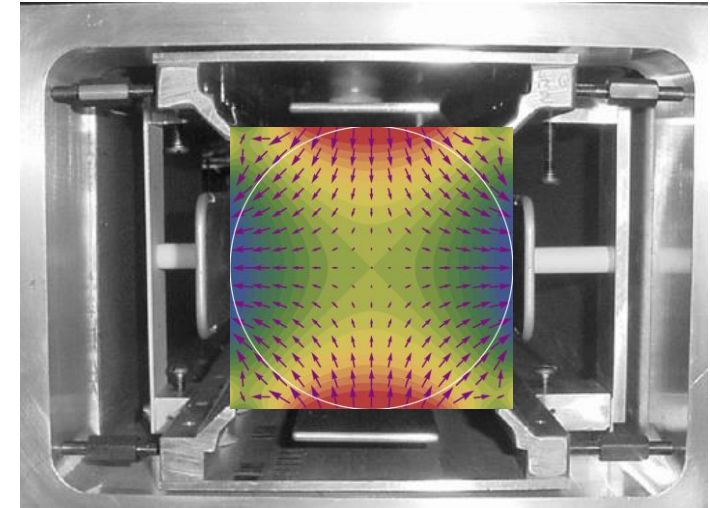
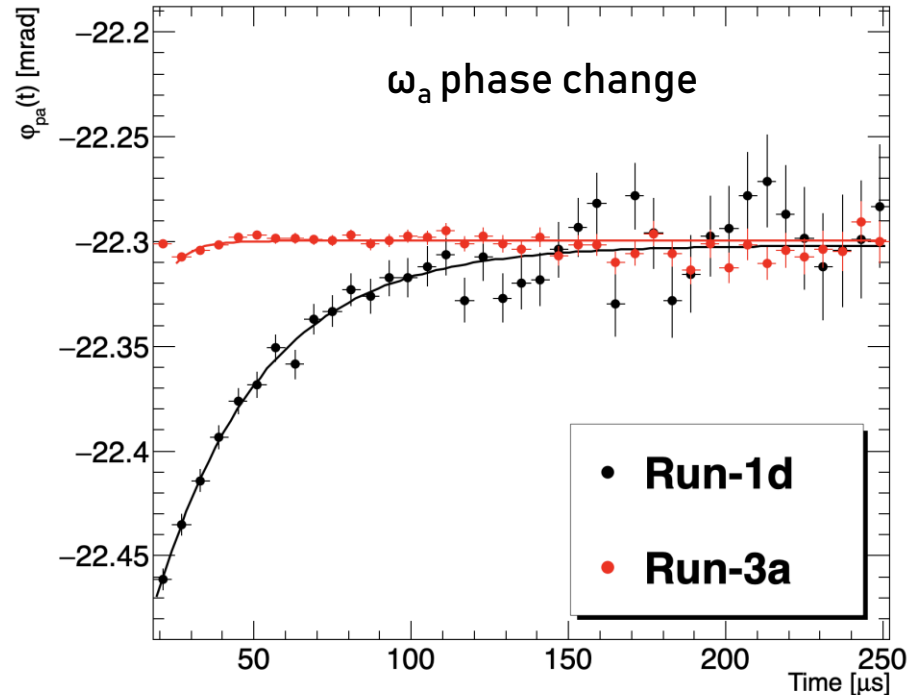
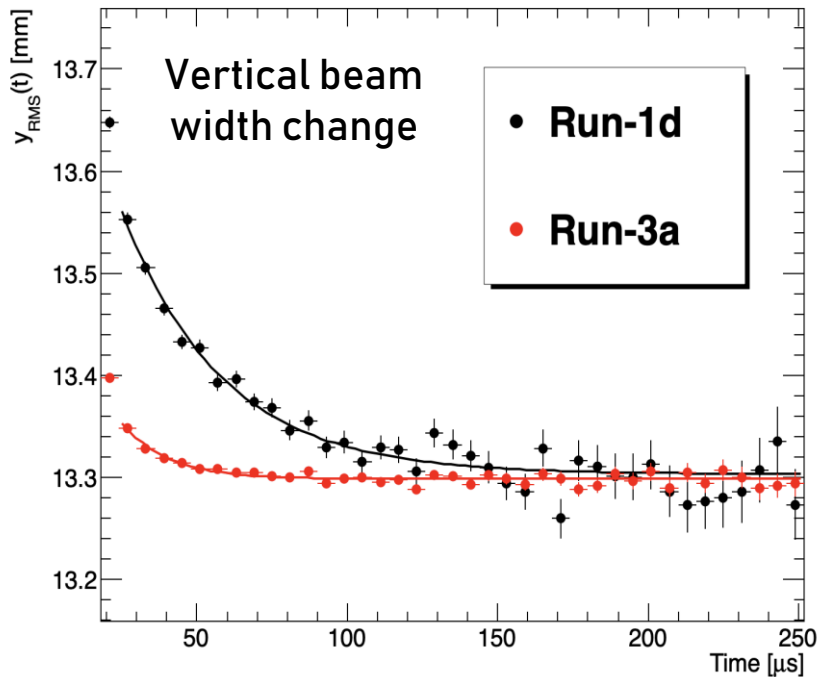


- Main reduction in uncertainty comes from better understanding of **transient field effects**
- Interpolation uncertainty has also reduced with **number of trolley runs**
- **Uncertainty already at TDR goal**

Improvements between Run-1 and Run-2/3

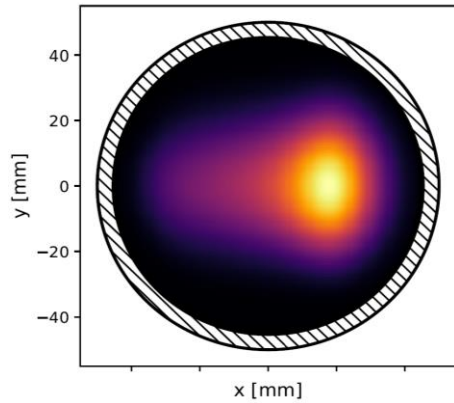
Damaged resistors

- In Run-1, 2 out of 32 resistors damaged in quad plates
→ unstable beam storage
- Redesigned and replaced before Run-2
- Reduces phase acceptance (C_{pa}) uncertainties 75ppb → 13 ppb
- Beam oscillation frequencies also become more stable

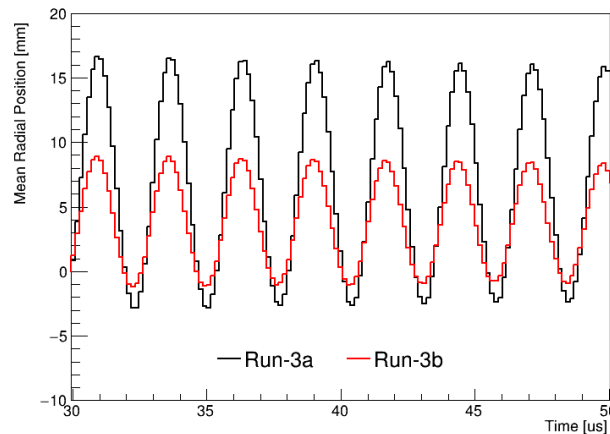
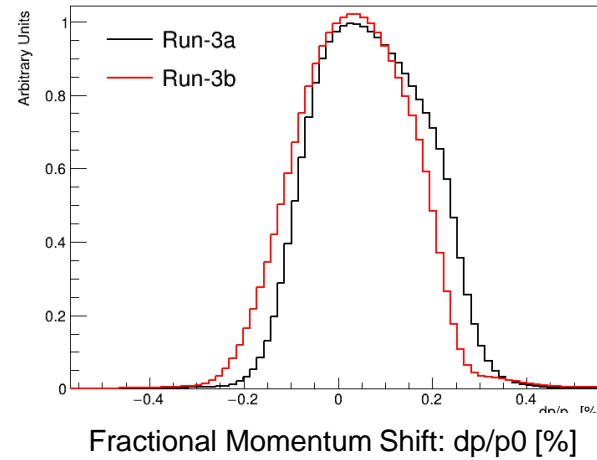
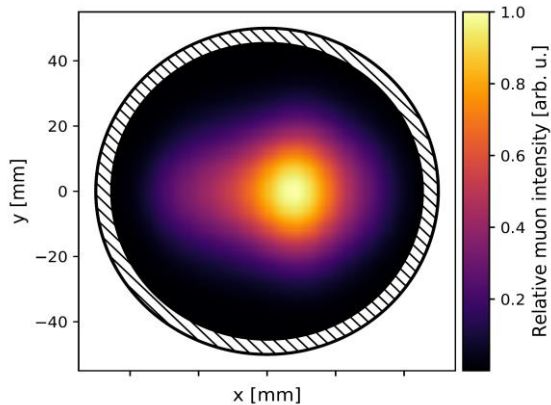


Kicker strength upgrade

Run 1 beam

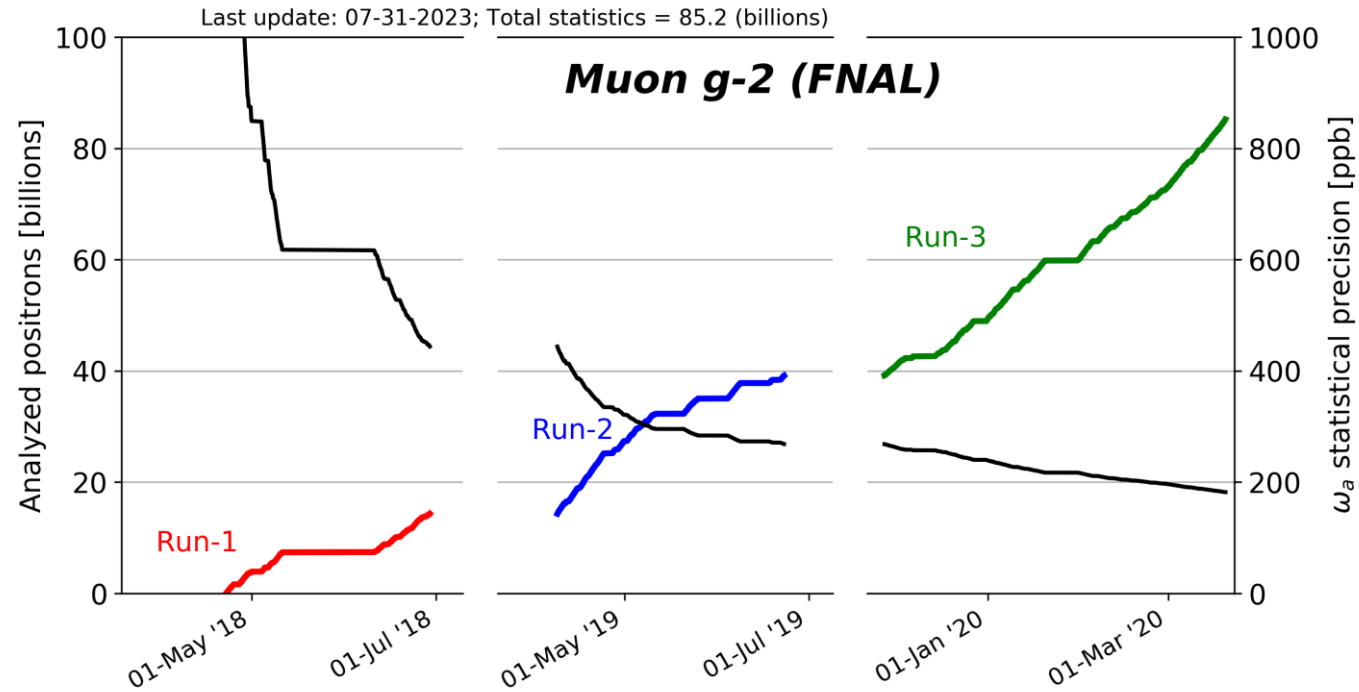


Late Run 3 beam



- Upgraded kicker cables while Run-3 so kicker can run at nominal strength
- Muon distribution more centered
 - **All systematics related to asymmetric beam shape reduced**
- Muon momentum distribution better centered on magic momentum
 - **E field correction reduced**
- Phase space matching improved
 - **Smaller beam oscillations**

Statistical improvement: Run-2/3 vs Run-1

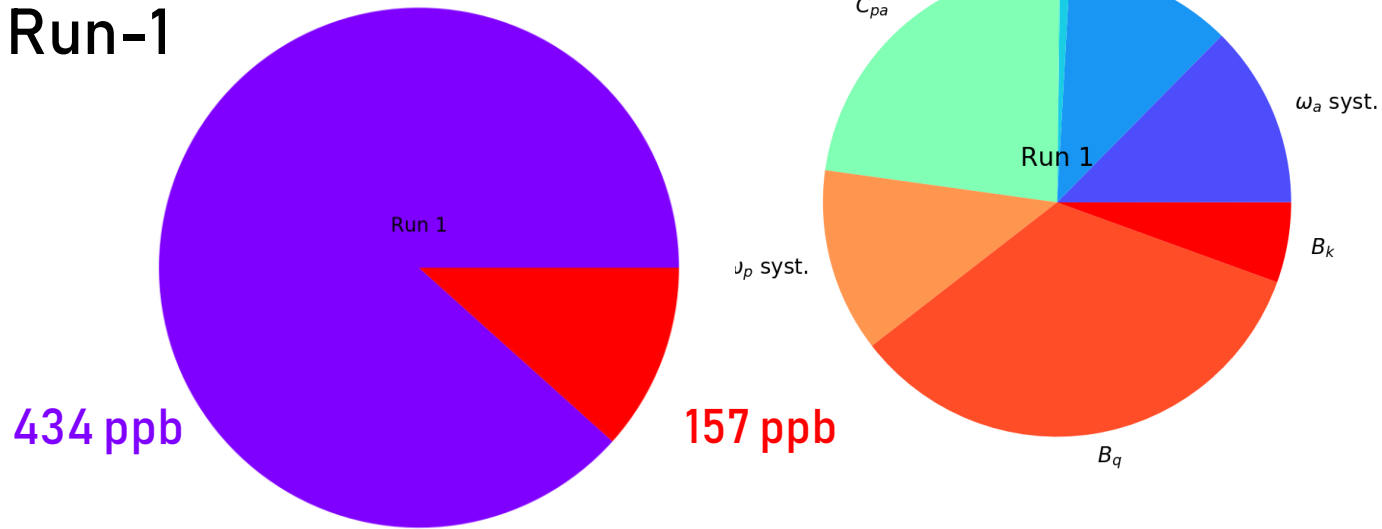


Dataset	Statistical Error [ppb]
Run-1	434
Run-2/3	201
Run-1 + Run-2/3	185

Total uncertainty

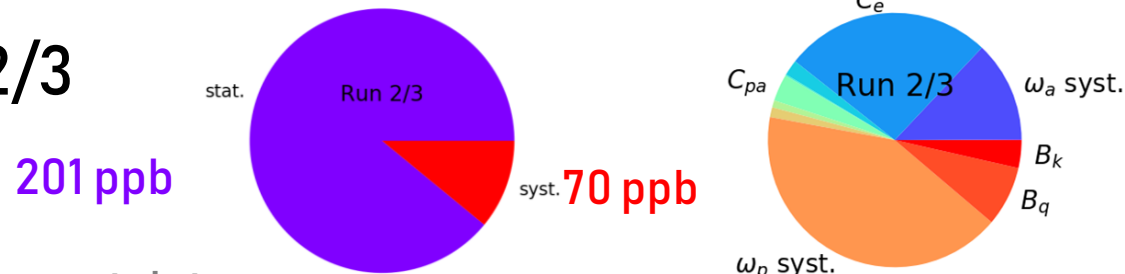
Total uncertainty: 462 ppb

Run-1



Total uncertainty: 215 ppb

Run-2/3

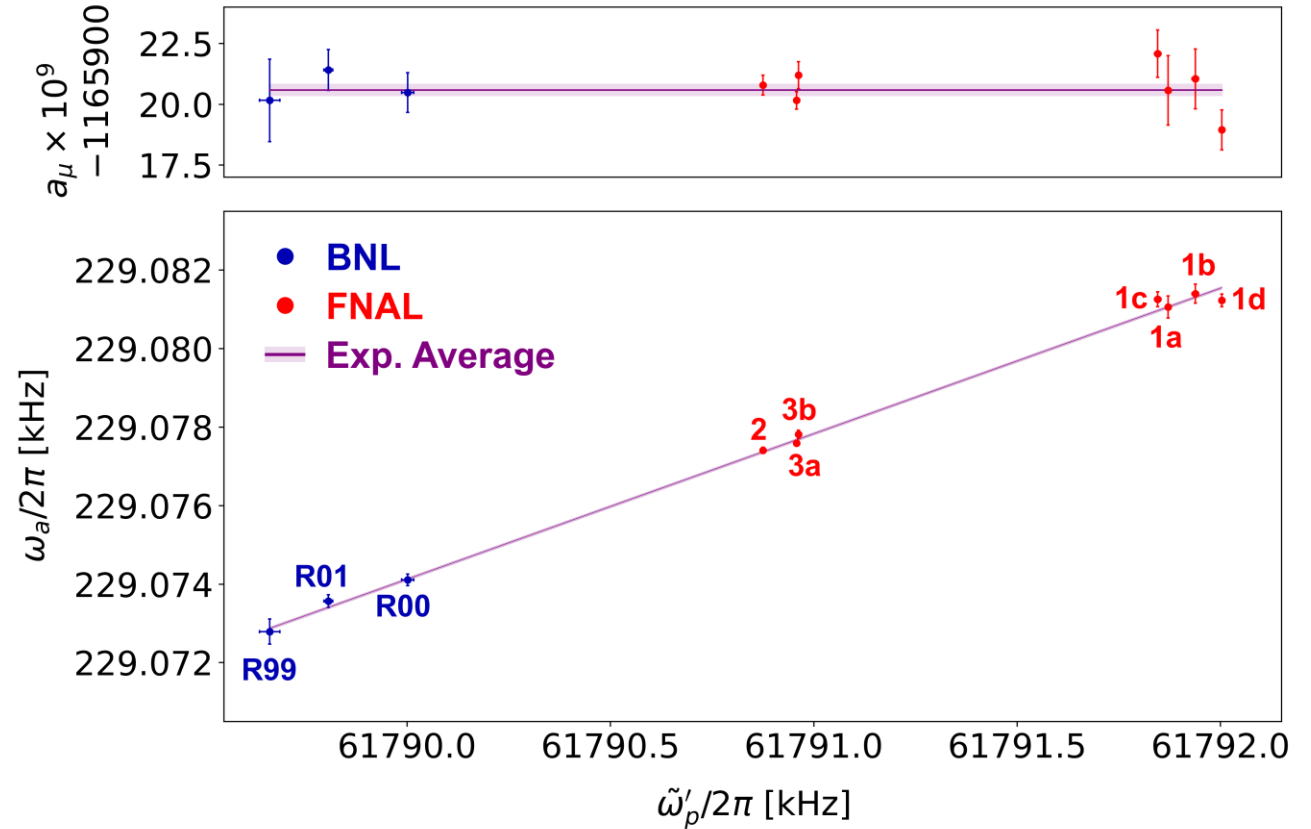
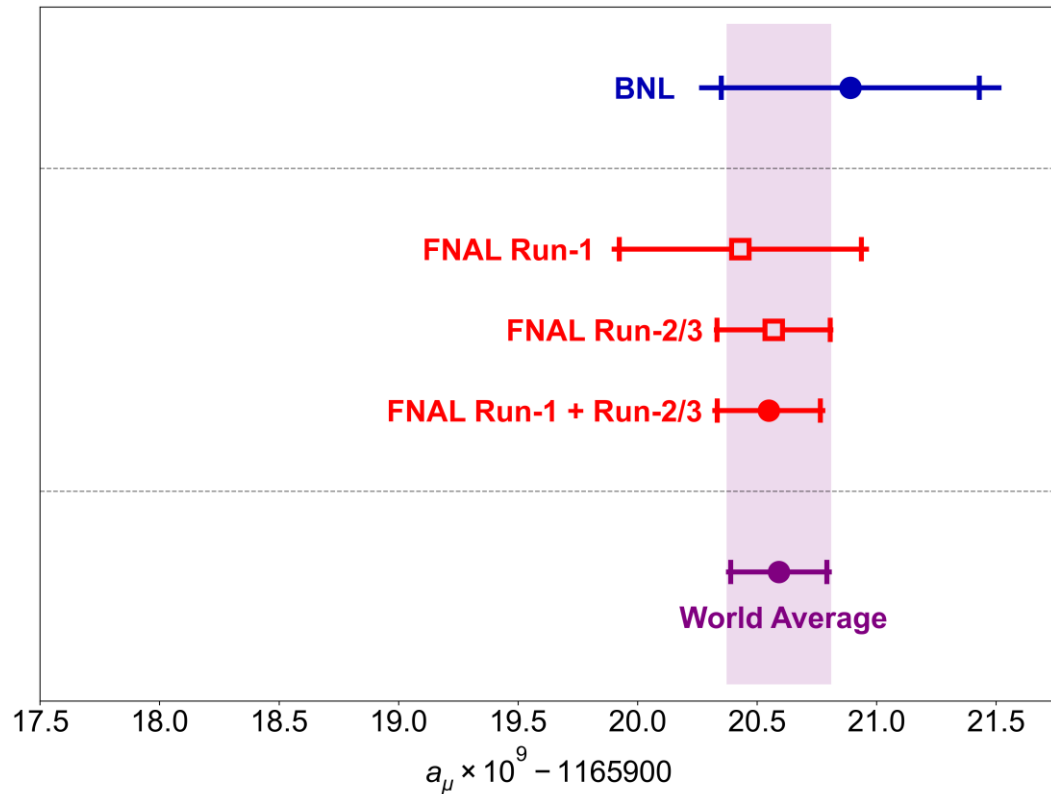


Radius: uncertainty

Area: variance

- Uncertainty reduced by factor >2
- Statistic and systematic uncertainty reduced by similar amount
- Systematic uncertainty below TDR goal
- Still statistics dominated

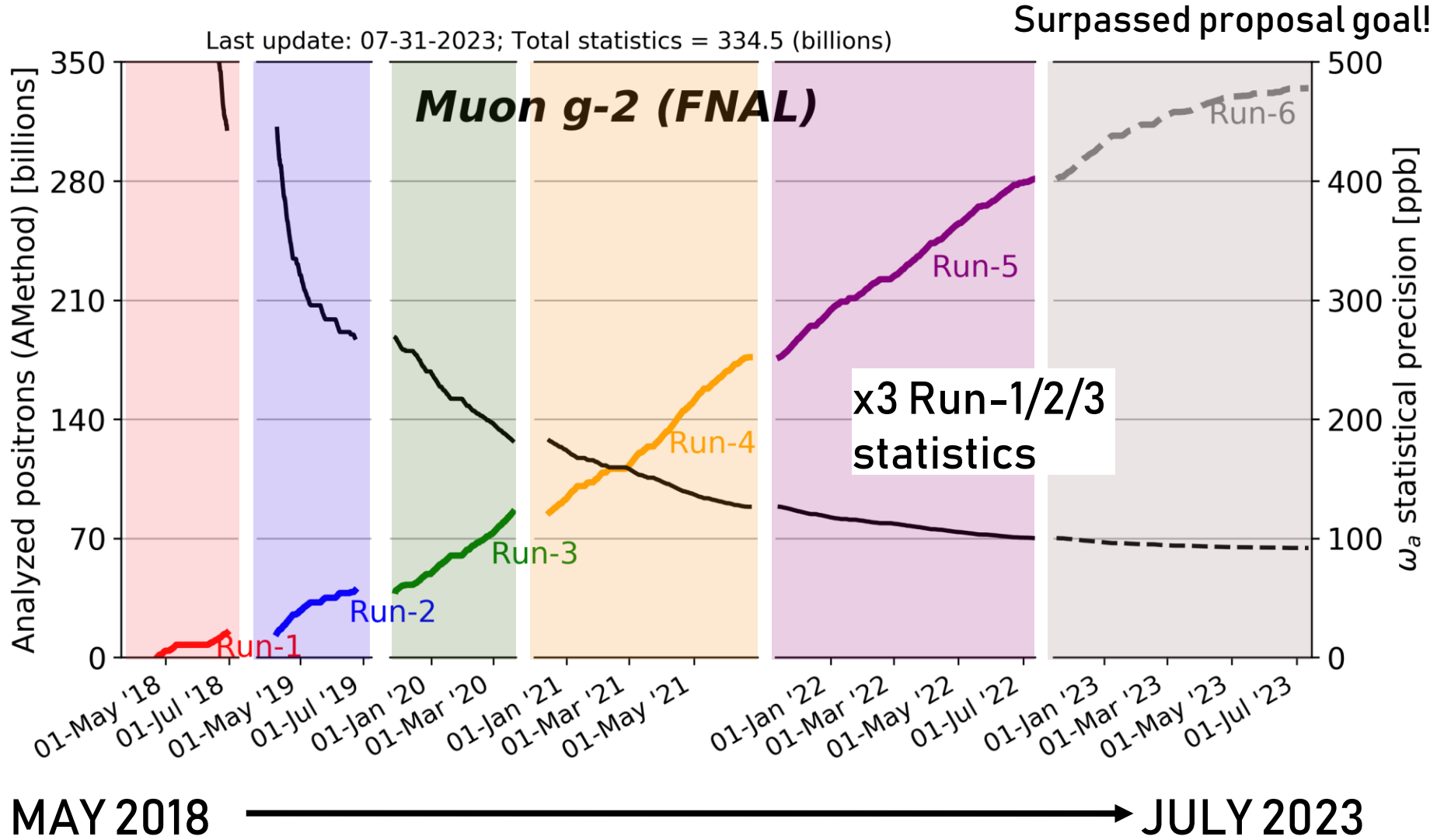
Unblinded result & cross-checks



$a_\mu(\text{Run-1}) =$	$0.00\ 116\ 592\ 040(54)$	$[463\ \text{ppb}]$
$a_\mu(\text{Run-2/3}) =$	$0.00\ 116\ 592\ 057(25)$	$[215\ \text{ppb}]$
$a_\mu(\text{FNAL}) =$	$0.00\ 116\ 592\ 055(24)$	$[203\ \text{ppb}]$
$a_\mu(\text{Exp}) =$	$0.00\ 116\ 592\ 059(22)$	$[190\ \text{ppb}]$

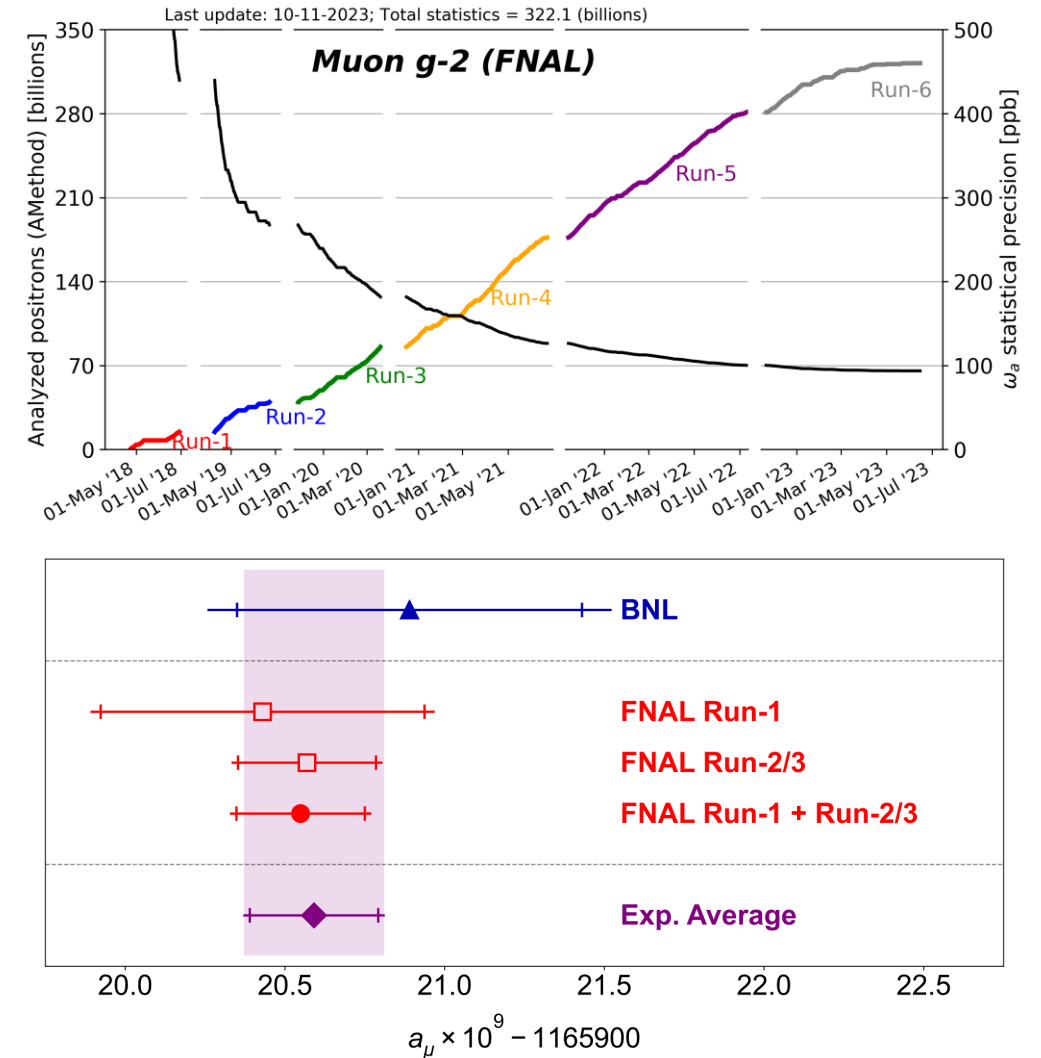
- Different runs performed at different magnet set-points – a useful consistency check
- Also divide datasets by other variables to check consistency (e.g. day/night, temperature, etc)

Beyond Run-2/3 : Total statistics



Conclusions

- High precision measurements of Muon $g-2$ stringent test on SM theory
- Run-2/3 data consistent with Run-1 and BNL
- Factor >2 in statistical and systematic uncertainty
- Surpassed TDR goals in statistics and systematics
- First time a three-way comparison of a_μ is possible (dispersive-approach, lattice approach, experiment)
- Another reduction by factor of 2 in statistical uncertainty from Run-4/5/6
- Expect final **result in 2025**



Phys. Rev. Lett. **131**, 161802 – Published 17 October 2023

Thank you!



Acknowledgements

- ▶ Department of Energy (USA)
- ▶ National Science Foundation (USA)
- ▶ Istituto Nazionale di Fisica Nucleare (Italy)
- ▶ Science and Technology Facilities Council (UK)
- ▶ Royal Society (UK)
- ▶ Leverhulme Trust (UK)
- ▶ European Union's Horizon 2020
- ▶ Strong 2020 (EU)
- ▶ German Research Foundation (DFG)
- ▶ National Natural Science Foundation of China
- ▶ MSIP, NRF, and IBS-R017-D1 (Republic of Korea)

